AD-A141 735 CONCRETE BEHAVIOR UNDER DYNAMIC TENSILE-COMPRESSIVE LOAD(U) ARMY ENGINEER WATERWAYS EXPERIMENT STATION VICKSBURG MS STRUCTURES LAB P F MLAKAR ET AL. JAN 84 WES/TR/SL-84-1 1/1

UNCLASSIFIED F/G 11/2 NL

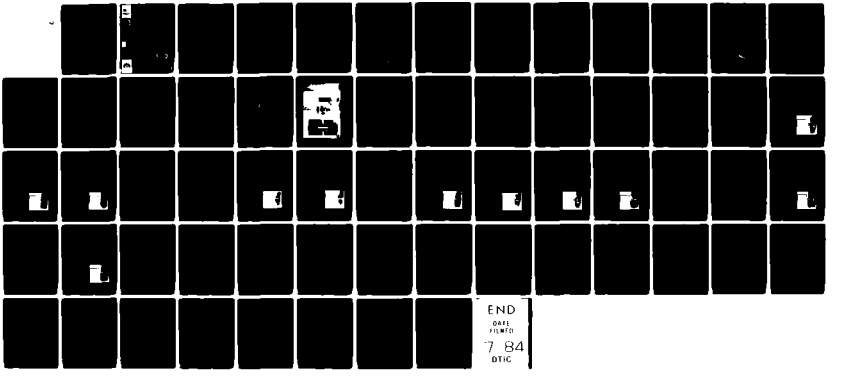

END
DATE FILMED
7 84
DTIC

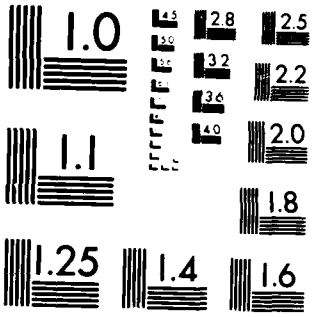

US Army Corps of Engineers

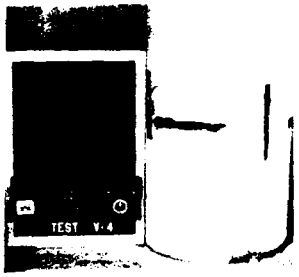

STRUCTURES LABORATORY

TECHNICAL REPORT SL-84-1

(12)

CONCRETE BEHAVIOR UNDER DYNAMIC TENSILE-COMPRESSIVE LOAD

by

Paul F. Mlakar, Ken P. Vitaya-Udom, Robert A. Cole

Structures Laboratory
U. S. Army Engineer Waterways Experiment Station
P. O. Box 631, Vicksburg, Miss. 39180

January 1984

Final Report

Prepared for Office, Chief of Engineers, U. S. Army
Washington, D. C. 20314

Destroy this report when no longer needed. Do not return it to the originator.

The findings in this report are not to be construed as an official Department of the Army position unless so designated by other authorized documents.

The contents of this report are not to be used for advertising, publication, or promotional purposes. Citation of trade names does not constitute an official endorsement or approval of the use of such commercial products.

Unclassified

SECURITY CLASSIFICATION OF THIS PAGE (When Data Entered)

REPORT DOCUMENTATION PAGE	READ INSTRUCTIONS BEFORE COMPLETING FORM
1. REPORT NUMBER: Technical Report SL-84-1	2. GOVT ACCESSION NO.: AD-A141735
	3. RECIPIENT'S CATALOG NUMBER
4. TITLE (and Subtitle): CONCRETE BEHAVIOR UNDER DYNAMIC TENSILE-COMPRESSIVE LOAD	5. TYPE OF REPORT & PERIOD COVERED: Final report
	6. PERFORMING ORG. REPORT NUMBER
7. AUTHOR(s): Paul F. Mlakar, Ken P. Vitaya-Udom, Robert A. Cole	8. CONTRACT OR GRANT NUMBER(s)
9. PERFORMING ORGANIZATION NAME AND ADDRESS: U. S. Army Engineer Waterways Experiment Station, Structures Laboratory, P. O. Box 631, Vicksburg, Miss. 39180	10. PROGRAM ELEMENT, PROJECT, TASK AREA & WORK UNIT NUMBERS
11. CONTROLLING OFFICE NAME AND ADDRESS: Office, Chief of Engineers, U. S. Army, Washington, D. C. 20314	12. REPORT DATE: January 1984
	13. NUMBER OF PAGES: 58
14. MONITORING AGENCY NAME & ADDRESS(if different from Controlling Office)	15. SECURITY CLASS. (of this report): Unclassified
	15a. DECLASSIFICATION/DOWNGRADING SCHEDULE

16. DISTRIBUTION STATEMENT (of this Report)

Approved for public release; distribution unlimited.

17. DISTRIBUTION STATEMENT (of the abstract entered in Block 20, if different from Report)

18. SUPPLEMENTARY NOTES

Available from National Technical Information Service, 5285 Port Royal Road, Springfield, Va. 22161.

19. KEY WORDS (Continue on reverse side if necessary and identify by block number)

Concrete
Dynamic response
Seismic analysis
Triaxial response

20. ABSTRACT (Continue on reverse side if necessary and identify by block number)

The significance of the dynamic biaxial material behavior of concrete in the study of structural response to seismic and other dynamic loadings is noted. A testing procedure is developed to examine this behavior for the case of monotonic, tensile-compressive loadings. The results of experiments for load ratios between uniaxial compression and uniaxial tension in which the time of application spanned from 10 min to 25 msec are presented. The tensile stress at failure is seen to decrease with an increase of the simultaneously

(Continued)

DD FORM 1 JAN 73 1473 EDITION OF 1 NOV 65 IS OBSOLETE

Unclassified

SECURITY CLASSIFICATION OF THIS PAGE (When Data Entered)

20. ABSTRACT (Continued).

acting compressive stress. The strength is observed to increase as the loads act more quickly, but the strains at failure are invariant with respect to loading time.

PREFACE

This study was conducted between 1978 and 1983 by personnel of the U. S. Army Engineer Waterways Experiment Station (WES) under the sponsorship of the Directorate of Civil Works of the Office, Chief of Engineers, U. S. Army. The work was funded under the Structural Engineering Research Work Unit 31588 which was monitored by Mr. Lucian G. Guthrie.

The investigation was conducted under the supervision of Messrs. Byrant Mather, Chief, Structures Laboratory (SL), William J. Flathau, Assistant Chief, SL, and James T. Ballard, Chief, Structural Mechanics Division, SL. Mr. Kenneth L. Saucier designed the constituents of the concrete mixture and controlled its production. Messrs. Darryl F. Hale and Billy W. Benson assisted in conducting the tests while Messrs. Frederick P. Leake, Jr., and William C. Strahan, Jr., instrumented them.

The Commanders of WES during the investigation and the preparation of this report were COL John L. Cannon, CE, COL Nelson P. Conover, CE, and COL Tilford C. Creel, CE. The Technical Director was Mr. F. R. Brown.

CONTENTS

CONVERSION FACTORS, NON-SI TO METRIC (SI) UNITS OF MEASUREMENT

Non-SI units of measurement used in this report can be converted to SI (metric) units as follows:

Multiply	By	To Obtain
degrees Fahrenheit	$t°C = (t°F - 32)/1.8$	degrees Celsius
feet	0.3048	metres
inches	2.54	centimetres
microinches per inch	1.0	micrometres per metre
pounds (force) per square inch	6.89476	kilopascals
pounds (force) per cubic foot	16.01846	kilograms per cubic metre
pounds (force) per cubic yard	0.59327642	kilograms per cubic metre

CONCRETE BEHAVIOR UNDER DYNAMIC TENSILE-COMPRESSIVE LOAD

CHAPTER 1

INTRODUCTION

1.1 BACKGROUND

The Corps of Engineers is directly responsible for the seismic safety of many concrete gravity dams and by its practice influences the safety of many more structures it owns. To fulfill this responsibility economically, the strength and stress-strain behavior of mass concrete under the multiaxial and dynamic states of stress induced by earthquake motions must be known. This report describes an investigation undertaken to improve the knowledge of this behavior. The results should also be of some value in assessing the response of various concrete structures to blast, wave, wind, and other dynamic loadings.

1.2 PREVIOUS RESEARCH

During a strong motion earthquake, it is generally believed that the individual monoliths of a concrete gravity dam will vibrate independently of one another (Chopra 1978). Accordingly, the mass concrete of each monolith is subjected to a nonuniform dynamic stress, which can be approximated by a plane stress condition. It follows that an understanding of mass concrete material behavior under such conditions is a prerequisite for any assessment of a gravity dam's seismic safety. Furthermore, the available information on the dynamic properties of structural concrete should be reviewed as well. Although structural concrete does not possess the thermal cracking problems during curing to the extent that mass concrete does, the stress-strain relations of the two materials appear to be similar (ACI 1963, 1970)."

Both the uniaxial and even the biaxial material behavior of concrete seems to be reasonably understood under statically applied loads. Accepted experiments have been conducted on thin plates loaded in plane (Kupfer, Hilsdorf, and Rusch 1969), on thin hollow cylinders loaded axially and by internal pressure (McHenry and Karni 1958), and on thin hollow cylinders loaded axially and in torsion (Bresler and Pister 1958, Goode and Helmy 1967). The results of these tests have established the biaxial stress combinations at which

concrete fails as well as its stress-strain behavior from no load through failure. Elastic, incrementally plastic theories of mechanical behavior have been subsequently proposed (Ottosen 1977, Chen and Chen 1975) which are consistent with and rationally generalize these experimental results, as shown in Figure 1.1.

The dynamic material behavior of concrete has only been reported for uniaxial states of stress. A number of experiments on cylinders monotonically loaded in compression (Watstein 1953, Hatano and Tsutsumi 1959, Atchley and Furr 1967, Kirillov 1977) and in tension (Hatano 1960, Raphael 1975) have been reported. One can generally conclude from this work that the strength and stiffness of concrete increase with increasing strain rate while the failure strain is unaffected by the rate of straining, as seen in Figure 1.2. Some experiments have also been conducted on cylinders cyclically stressed in compression (Ban and Muguruma 1960, Hatano and Watanabe 1971, Takeda and Tachikawa 1973) and in tension (Saucier 1977). These results suggest that the strains at failure may be independent of the history of stresses and strains.

However, no experimental information has been published describing the biaxial, dynamic material properties of concrete. An analytical thesis of concrete dam behavior, in which reasonable bounds for these unknown properties were assumed, suggests that the extent of cracking induced by seismic ground motion can be very sensitive to these assumptions (Pal 1974). Although these must eventually be defined under cyclic and reversible strains representative of earthquake induced vibrations, logically they must first be experimentally measured for monotonic loadings. These must also be known in all quadrants of the biaxial space. But an understanding of biaxial tension-compression behavior is the foremost concern, since the stress state of a dam's cracked regions occur in this quadrant.

1.3 SCOPE

Accordingly, the scope of this first experimental investigation of concrete dynamic, biaxial material behavior is confined to monotonic, tension-compression loadings. In the following chapters of this report, the experimental procedure will be detailed, the test results will be discussed, and suggestions for further study of this behavior will be offered.

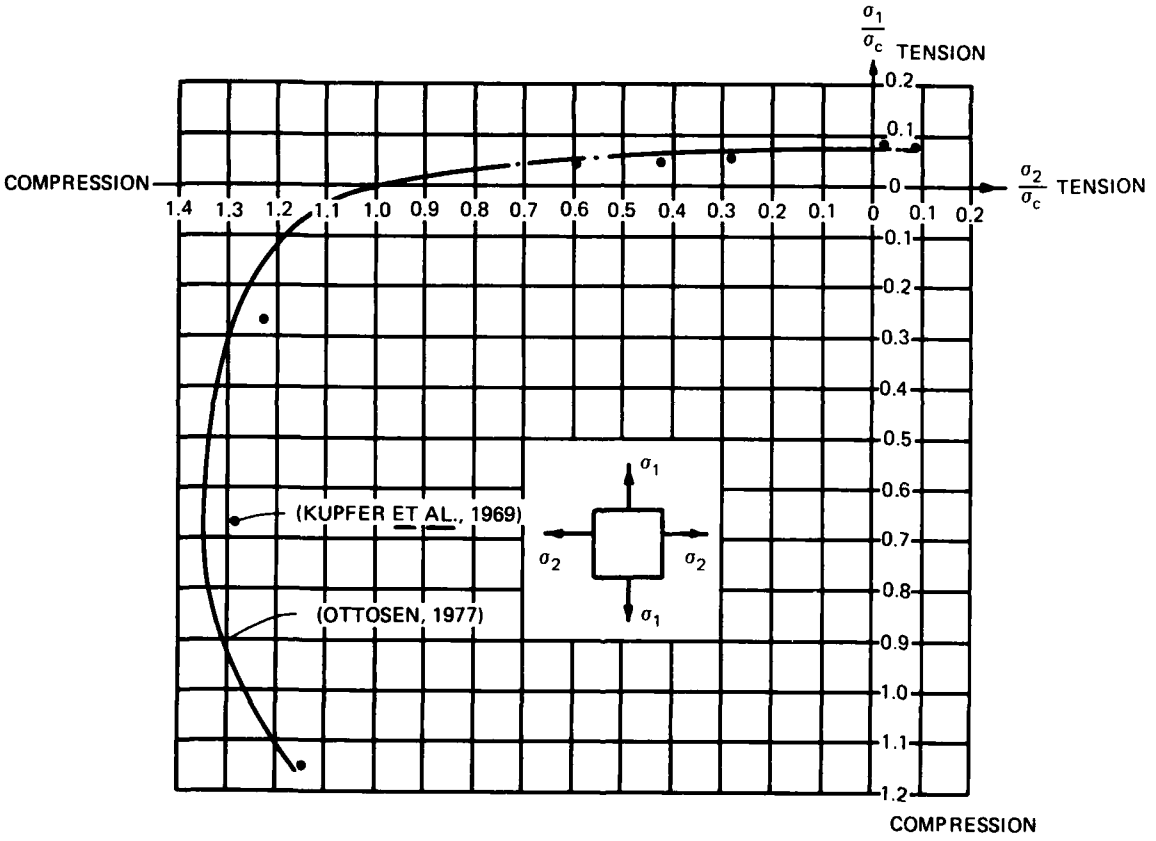

Figure 1.1 Static biaxial failure theory and experiment.

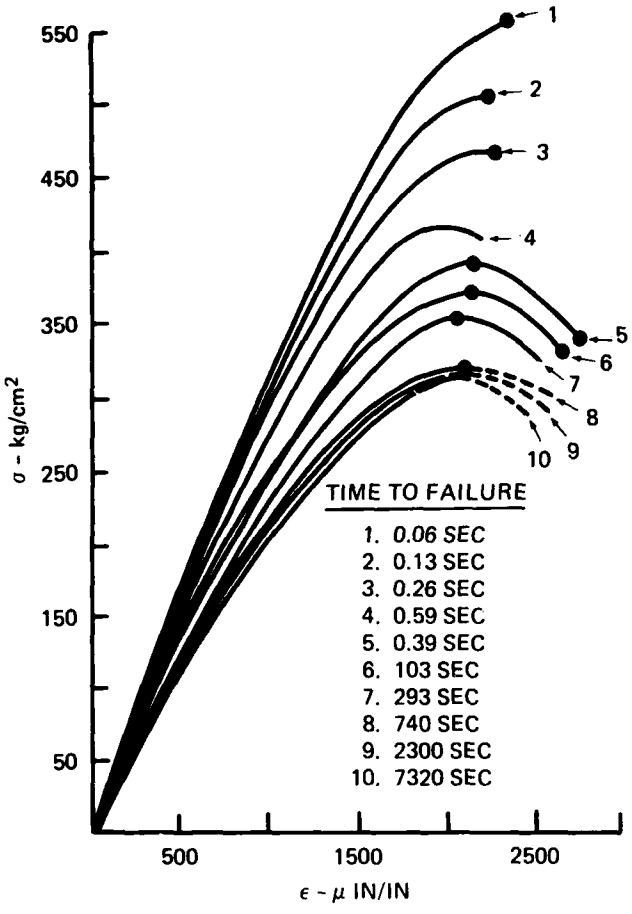

(a) COMPRESSION (HATANO & TSUTSUMI, 1959)

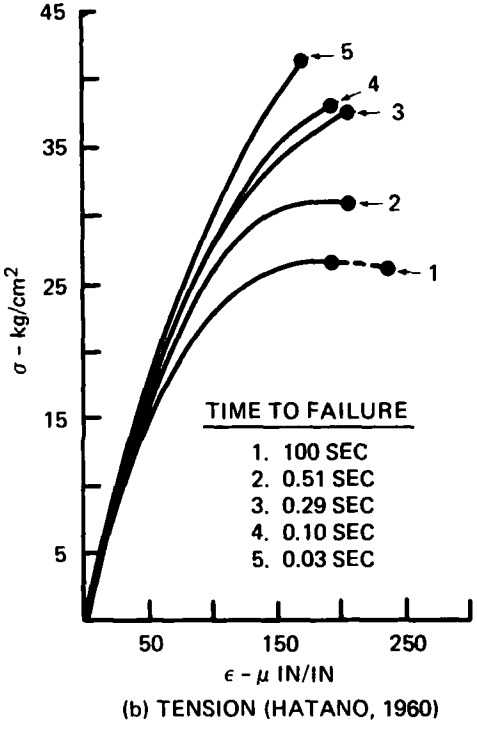

(b) TENSION (HATANO, 1960)

Figure 1.2 Dynamic uniaxial experiments.

CHAPTER 2

PROCEDURE

A number of techniques to measure the dynamic, biaxial material behavior were critically examined in the design of this experiment. These included thin square plates loaded in plane; hollow cylindrical specimens loaded by pressure, torque, and thrust; rhomboidal sandwich plates loaded anticlastically (having opposite curvatures); solid cylindrical specimens loaded radially and axially; and beams loaded laterally. The comparison concluded that practically significant data about monotonic, tensile-compressive properties could economically be gathered using hollow cylinders of 3000 psi,[a] 3/8-inch maximum size aggregate loaded in axial compression and internal pressure by a quickly modified hydraulic device existing at the WES.

2.1 SPECIMENS

As shown in Figure 2.1, the experimental specimen was a hollow right circular cylinder of 13-inch inner diameter, 1-inch wall thickness, and 26-inch height. The specimen's radius-to-wall thickness ratio, 6.5, is high enough to assure an elastic distribution of tensile hoop stress that is uniform to within 8 percent (Timoshenko 1941). Reasonable static results were reported in McHenry and Karni (1958), which were obtained from a similar specimen having a less uniform distribution corresponding to a radius-to-thickness ratio of 2.5. This study's height-to-outer diameter ratio matches that of McHenry and Karni (1958) to give a uniformly stressed central region uninfluenced by the boundary conditions at the ends of the specimen. This height is also small enough that the transit time (<0.2 ms (millisecond) for 155 lb/ft^3, 5 x 10^6 psi modulus concrete) for axial-stress waves is virtually instantaneous in comparison to the loading rise times of interest (>25 ms).

The constituents of concrete mixture used for these specimens are given in Table 2.1. This mixture was selected to have a nominal 90-day compressive strength of 3000 psi. The maximum aggregate size was restricted to 3/8 inch to duplicate the ratio of the parameter-to-specimen wall thickness used in McHenry and Karni (1958). The aggregate size distribution, shape, and mineral

---

[a] A table of factors for converting non-SI units of measurement to metric (SI) units is given on page 3.

content of this mix were otherwise chosen to be as representative as possible of mass concrete. All cement and aggregates for all the specimens were blended together in a single common dry batch to minimize the variation of concrete strength among the lots of specimens.

The specimens were cast in lots of five, in steel molds, mounted on a vibrating table. These molds were removed after 48 hours and prepared for reuse. The specimens were then cured until 28 days old in a fog room. Thereafter, until testing at approximately 90 days age, the specimens were sealed within plastic bags at ambient temperatures less than 85°F. Before each test, the inside surface of the cylinder was thinly coated with an epoxy to prevent the intrusion of water into the wall, under pressure. An epoxy cap was also cast at both ends of the cylinder to provide a smooth surface for the O-ring seals, as shown in Figure 2.1.

2.2 LOADING

All loadings were applied by the WES 200 kip-loader (shown in Figure 2.2) which can apply monotonic loadings with rise times as fast as 1 ms (Balsara and Hossley 1973). This simple and inexpensive open-loop hydraulic device employs a silicone oil as the working fluid. Static loads are applied by slowly pressurizing the upper chamber while maintaining little or no pressure in the lower chamber. Dynamic loads are generated by pressurizing the upper chamber to a level greater than the lower one and then suddenly releasing the fluid through the orifice shown. The shape of the loading-versus-time curve thus created is obviously a complex function of fluid pressure, fluid volume, orifice opening, and specimen stiffness which cannot be controlled with absolute precision. However, it is possible to satisfactorily generate nominal peak loads and rise times after some preliminary calibrations.

The special aluminum fixtures, shown in Figure 2.1, were fabricated to mount the concrete specimens in the 200-kip loading device. The top fixture incorporated two valved openings so that the specimen could be filled with water in such a way that no significant air was entrapped. The bottom fixture contained mounts for two pressure transducers. A satisfactory seal between each fixture and the specimen was established with O-rings.

Thus, the hydraulic ram's loading was carried in part by an axial compression in the specimen and in part by a pressurization of the contained water, which simultaneously loaded the specimen in circumferential tension.

Three nominally different proportions of compressive and tensile loadings were achieved by inserting a 1/4-inch thick, a 1/16-inch thick, or no rubber pad between the top fixture and the specimen (Figure 2.1), so as to effectively change the relative stiffness of the two parallel load paths seen by the ram. A uniaxial compressive loading was also achieved by simply not filling the specimen with water. Finally, an essentially uniaxial tensile condition resulted when the specimen was overfilled so that the top fixture bore only on the water surface.

2.3 INSTRUMENTATION

The total load-versus-time function, applied by the hydraulic ram in each test, was measured by the load cell shown under the bottom fixture in Figure 2.3. The sensing element of this cell is a hollow column. Two axial and two transverse strain gages on this column were wired to form a fully active Wheatstone bridge circuit.

The water pressure inside each cylinder was independently measured by two identical pressure gages in the bottom fixture. Each gage's sensing element was a 0.1-inch-diameter steel diaphragm containing four semiconductor strain gages in a fully active four-arm Wheatstone bridge.

Three independent measurements each of axial strain, outer circumferential strain, and inner circumferential strain were made on each specimen, as shown in Figure 2.4. Each of these nine measurements was made with a single 6-inch-long, constantan alloy, wire gage.

The signals from all twelve of these channels were simultaneously recorded on FM magnetic tape during each test. A corresponding digital magnetic tape was subsequently produced for later reduction of these data, as described in Chapter 3.

2.4 CONTROL CYLINDERS

Six conventional 6-by-12-inch control cylinders were cast with each lot of hollow cylinders and were cured under the same conditions. Four of the control cylinders were statically tested in compression (ASTM C 39-72) to measure strength, axial strain, and transverse strain (ASTM 1972). The remaining two cylinders were statically tested in direct tension (ASTM D 2936-78) to measure strength and axial strain (ASTM 1978).

Table 2.1. Constituents of concrete mixture.

Constituent	lb/yd^3
Portland Cement, Type II	470
Sand, Limestone	1600
Rock, Limestone 3/8 in maximum	1600
Water	376

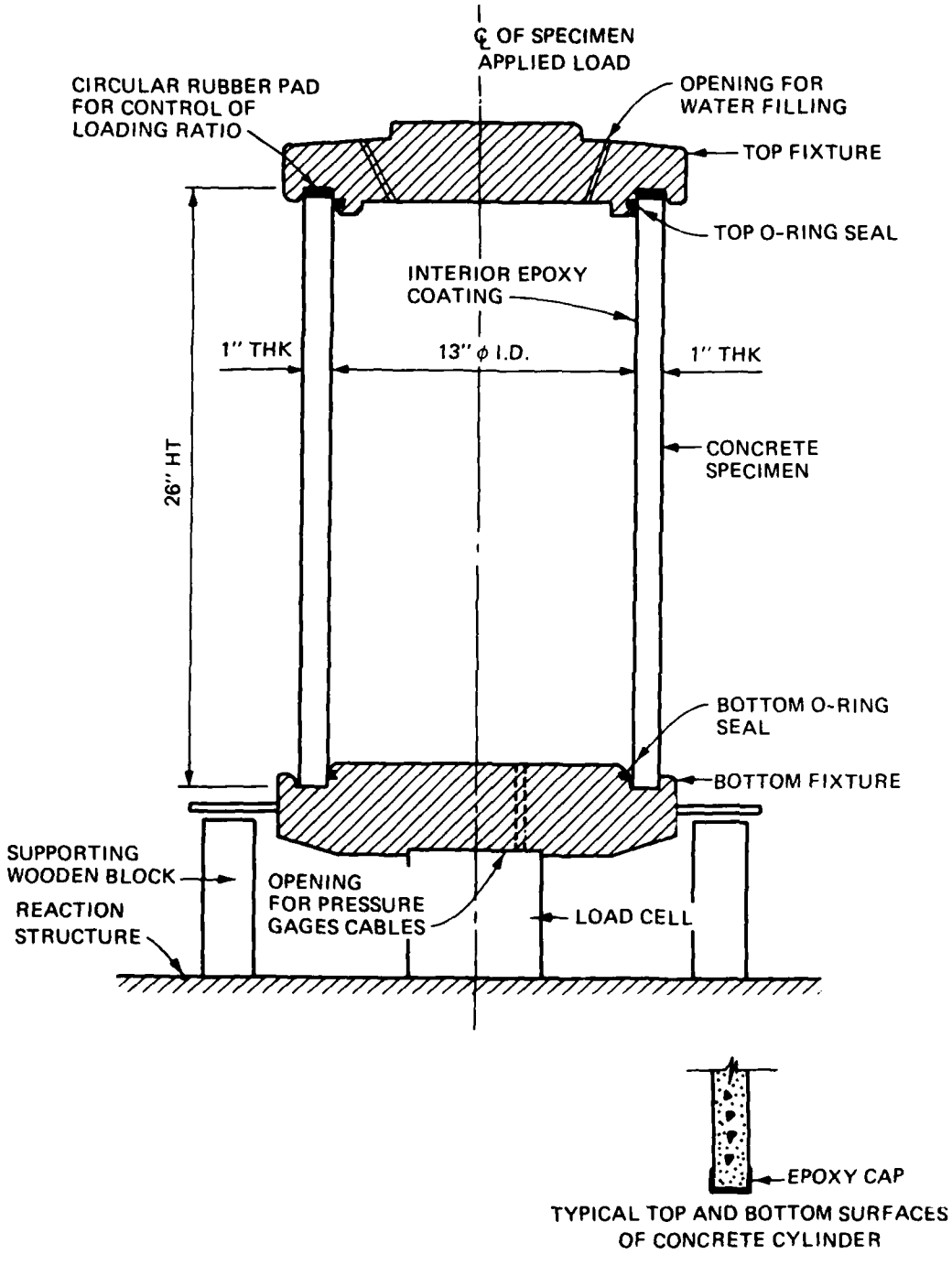

Figure 2.1 Biaxial test specimen and loading fixture.

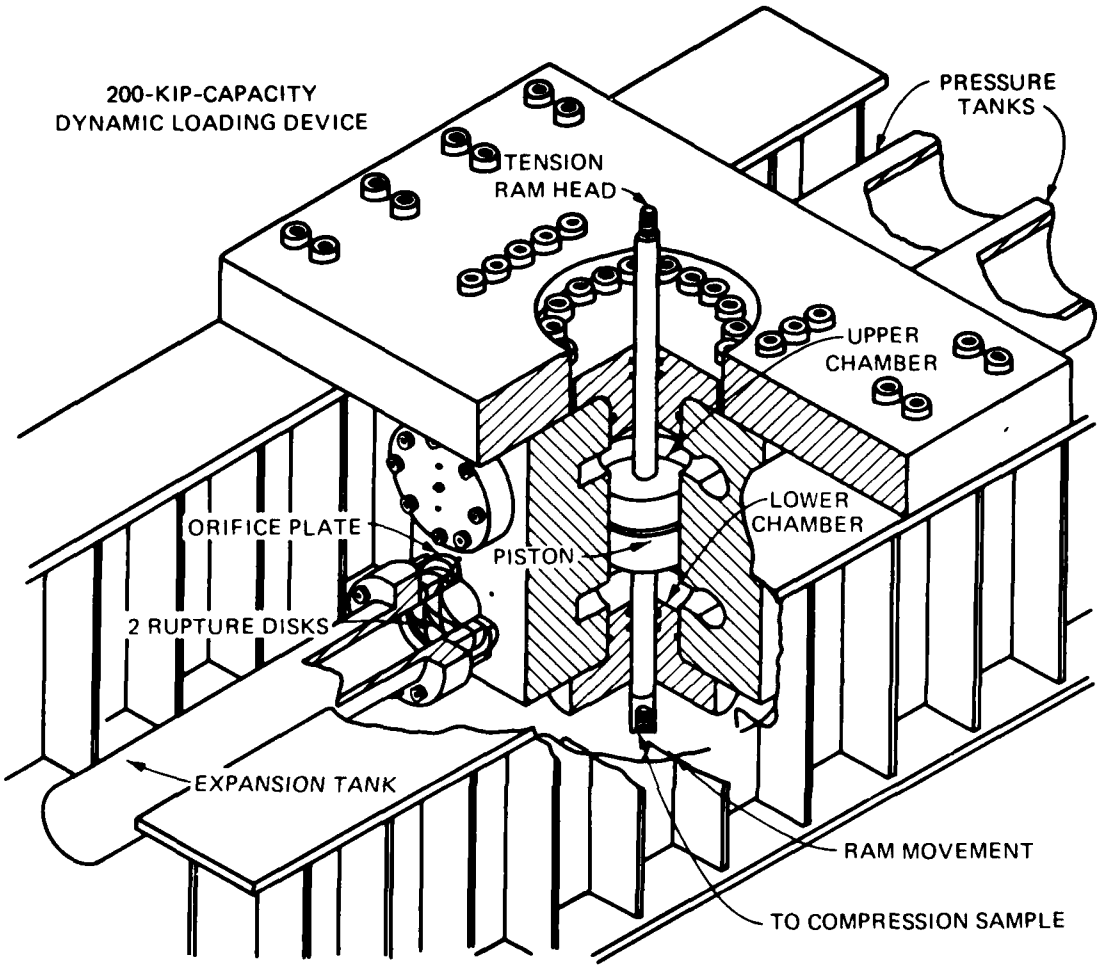

CHARACTERISTICS

1. PEAK DYNAMIC LOAD: 200,000 LB IN LESS THAN 2 MSEC
2. RISE TIME: 1 TO 200 MSEC
3. HOLD TIME: 0 TO 200 MSEC
4. DELAY TIME: 15 TO 500 MSEC

APPLICATIONS

1. DETERMINATION OF DYNAMIC STRESS-STRAIN PROPERTIES OF CONSTRUCTION MATERIALS
2. DYNAMIC TEST OF STRUCTURAL ELEMENTS:
   a. BEAMS UP TO 18 FEET IN LENGTH
   b. COLUMNS UP TO 8 FEET IN LENGTH
   c. TENSILE SPECIMENS UP TO 3 FEET IN LENGTH
   d. STRUCTURAL CONNECTIONS AND FRAMES

Figure 2.2 Cutaway view of 200-kip-capacity loader.

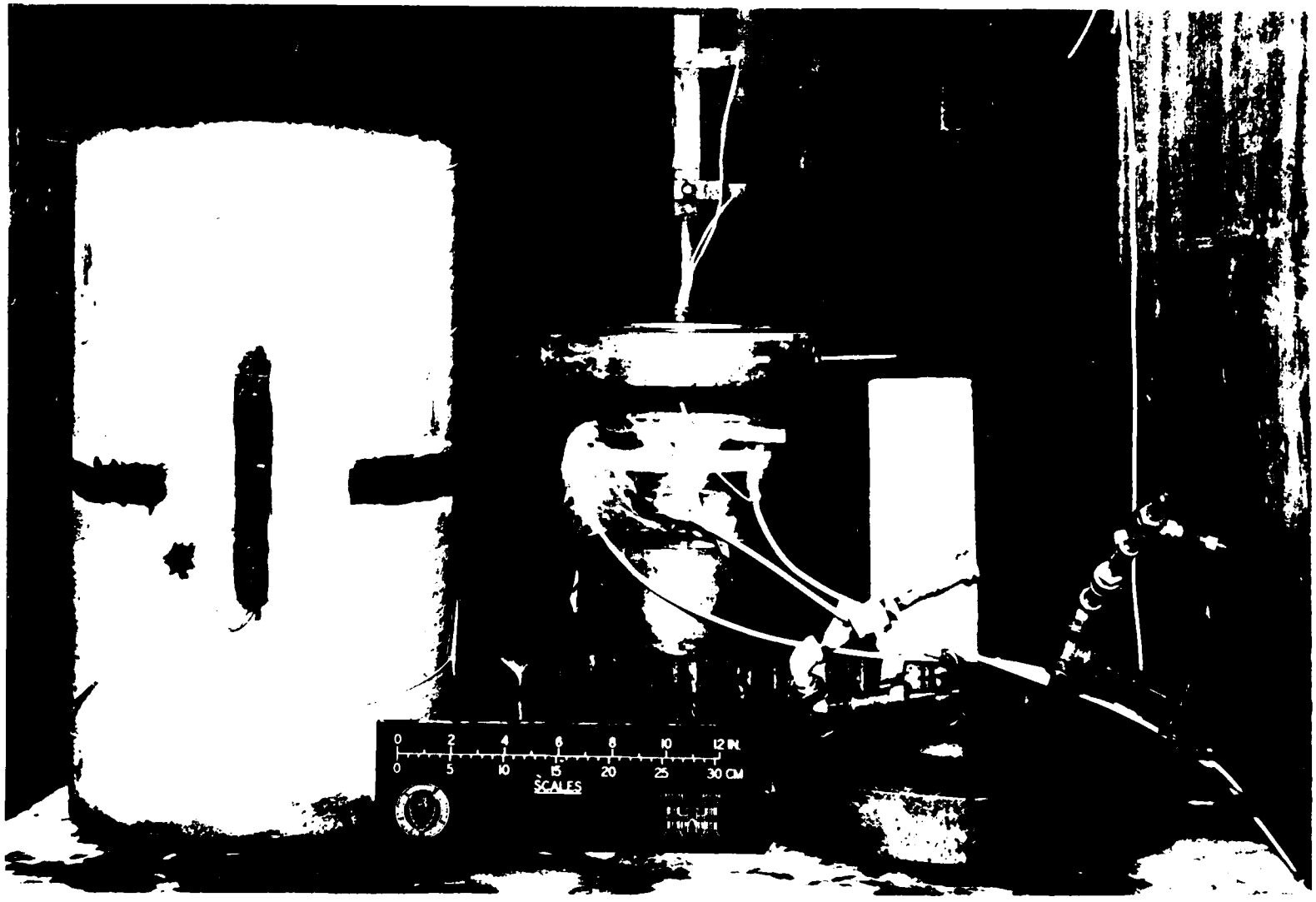

Figure 2.3 Typical test specimen and loading device.

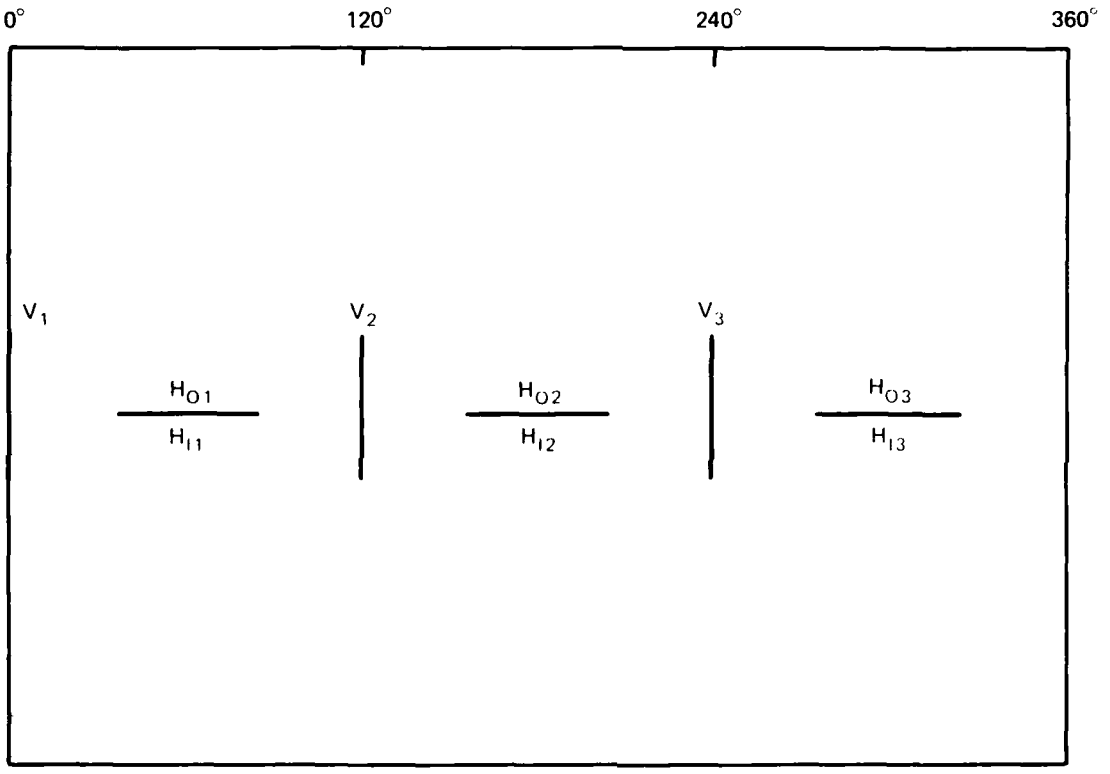

H_O - OUTSIDE SURFACE OF CONCRETE CYLINDER
H_I - INSIDE SURFACE OF CONCRETE CYLINDER

Figure 2.4 Location of strain gages.

CHAPTER 3

RESULTS

Eight lots of five hollow cylindrical specimens each were produced. Of these, twenty-nine appeared to be of adequate quality to test. Eleven of these tests were invalid because the specimen's state-of-stress did not appear to be uniform before failure. The dynamic, biaxial loading condition and the specimen lot of the 18 tests considered to be successful are listed in Table 3.1. These conditions include static, biaxial, and dynamic uniaxial states comparable to previously published results of other researchers, as well as dynamic, biaxial states heretofore untested.

For each test, the data recorded on magnetic digital tape were reduced with the aid of the WES central computer system as follows. Individual plots of the load cell, the two pressure transducers, and the nine strain gages (as a function of time) were first examined to eliminate invalid recordings. The compressive stress function of time $\sigma_c(t)$ was then computed by dividing the net force carried in the cylinder wall by its cross-sectional area, i.e.

$$\sigma_c(t) = \frac{P(t) - \pi r_i^2 p(t)}{\pi(r_o^2 - r_i^2)}$$

in which

$P(t)$ = load function measured by load cell

$p(t)$ = average of valid pressure transducer measurements

r_i = specimens inner radius (6.5 inches)

r_o = specimens outer radius (7.5 inches)

The tensile stress was calculated from the thin-walled approximation (Timoshenko 1941):

$$\sigma_t(t) = \frac{r_i}{r_o - r_i} p(t)$$

The compressive $\varepsilon_c(t)$, outer tensile $\varepsilon_{to}(t)$, and inner tensile $\varepsilon_{ti}(t)$ strain functions of time were estimated by the mean of the valid measurements of each strain.

These results are shown in Figures 3.1 through 3.18. The (a) part of

each figure depicts the reference stress versus time function. This reference stress is the compressive stress $\sigma_c(t)$ except for the uniaxial tensile tests in which it is $\sigma_t(t)$. The (b) portion of each figure then shows how the other stress varied with respect to the reference stress. The strain behavior as a function of the reference stress is next presented in part (c). Finally the (d) part of each figure is a photograph of the failed specimen, if available.

From an examination of these plots, the magnitudes of compressive σ_c and tensile σ_t stress at failure were judged, as indicated for each specimen, and listed in Table 3.2. The time since load application at which this failure occurred t_r , the compressive strain magnitude ε_c , and the average ε_t of the inner and outer tensile strain magnitudes at failure are also presented in this listing. The last column qualitatively indicates whether the failure was "compressive" (accompanied by the complete disintegration of the specimen) or "tensile" (characterized by a single longitudinal cleavage).

The results of the 6- by 12-inch control cylinder tests appear in Table 3.3. For those specimens tested in static, uniaxial compression, the maximum stress σ_c and corresponding compressive ε_c and tensile ε_t strains are given. For the cylinders loaded in static, uniaxial tension, the maximum stress σ_t and corresponding strain ε_t are listed.

Table 3.1. Dynamic tension-compression test conditions.

Test[a,b]	Age Days	Lot
I-1	91	a
I-2	93	a
I-3	94	a
I-4	88	b
II-1	106	d
II-2	83	e
II-4	106	e
II-5	107	d
III-1	90	b
III-2A	98	d
III-4	84	c
III-4A	111	h
III-5	85	c
IV-1	112	d
IV-2	81	f
IV-3	112	h
V-1	93	g
V-4	96	g

[a]Dynamic conditions of 200-kip loader: I--Static; II--0.082-inch orifice with solenoid valve; III-0.182-inch orifice with solenoid valve; IV--0.4375-inch orifice with solenoid valve, and; V--1.1875-inch orifice with rupture disc.
[b]Biaxial conditions of loading fixture: 1--No water, no insert; 2--Water, no insert; 3--Water, 0.0625-inch insert; 4--Water, 0.25-inch insert, and; 5--Water, fixture off cylinder.

Table 3.2. Dynamic tension-compression test results.

Test	t_r ms	σ_c psi	σ_t psi	ε_c μin/in	ε_t μin/in	Type of Failure
I-1	600000*	3060	0	1340	440	Compressive
I-2	600000*	2620	50	742	158	Tensile
I-3	600000*	1180	145	265	88	Tensile
I-4	600000*	920	121	230	77	Tensile
II-1	1420	2600	0	1185	160	Compressive
II-2	1160	1920	35	480	110	Compressive
II-4	630	425	295	110	110	Tensile
II-5	273	0	372	15	105	Tensile
III-1	1070	3780	0	1055	500	Compressive
III-2A	440	2580	21	690	155	Tensile
III-4	54	26	340	20	60	Tensile
III-4A	102	270	305	80	100	Tensile
III-5	170	58	325	40	65	Tensile
IV-1	69	2530	0	790	220	Compressive
IV-2	188	2840	73	990	385	Compressive
IV-3	50	1080	350	280	150	Tensile
V-1	25	3700	0	1240	355	Compressive
V-4	270	500	440	120	205	Tensile

* Static.

Table 3.3. Static control cylinder test results.

Lot	Specimen	σ_c psi	σ_t psi	ε_c μin/in	ε_t μin/in	Lot	Specimen	σ_c psi	σ_t psi	ε_c μin/in	ε_t μin/in
a	1	3520		2050	800	e	25	3100		2200	700
	2	3630		1950	700		26	3080		2100	1000
	3	3450		2100	1300		27	3130		2200	1000
	4	3570		2100	900		28	3110		2100	750
	5		290		60		29		340		95
	6		320		60		30		375		100
b	7	3710		2350	1100	f	31	3020		2300	1000
	8	3700		2150	1000		32	3100		2550	1250
	9	3500		2200	1000		33	2880		2550	1000
	10	3590		2300	1200		34	2940		2450	880
	11		310		65		35		320		90
	12		230		55		36		360		90
c	13	3540		2500	900	g	37	3250		2050	1400
	14	3400		2100	700		38	3270		2150	800
	15	3430		2400	950		39	3220		2300	1200
	16	3430		2500	900		40	3180		2150	1100
	17		305		70		41		250		60
	18		335		85		42		255		60
d	19	3560		2300	1250	h	43	3250		2600	1500
	20	3590		2300	900		44	3200		2200	1000
	21	3430		2300	900		45	3020		2300	1000
	22	3660		2200	1000		46	3180		2300	1000
	23		245		55		47		390		90
	24		360		95		48		270		85

Static

Uniaxial

a. Dynamic load

b. Biaxial load

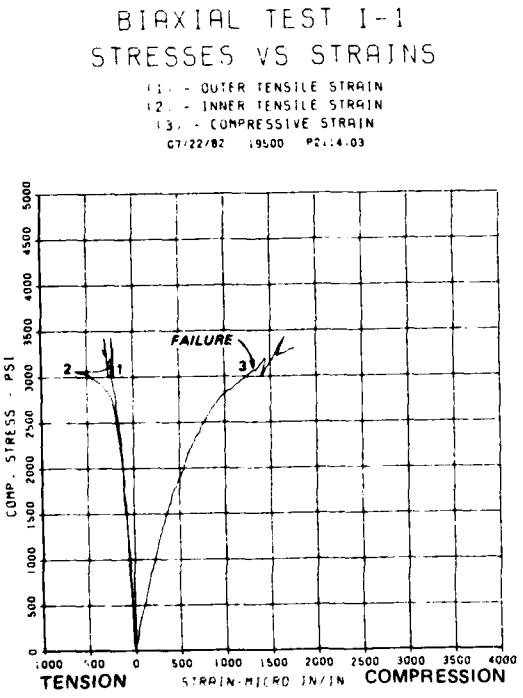

Disintegrated

c. Strain

d. Failed specimen

Figure 3.1 Results of Test I-1.

Static

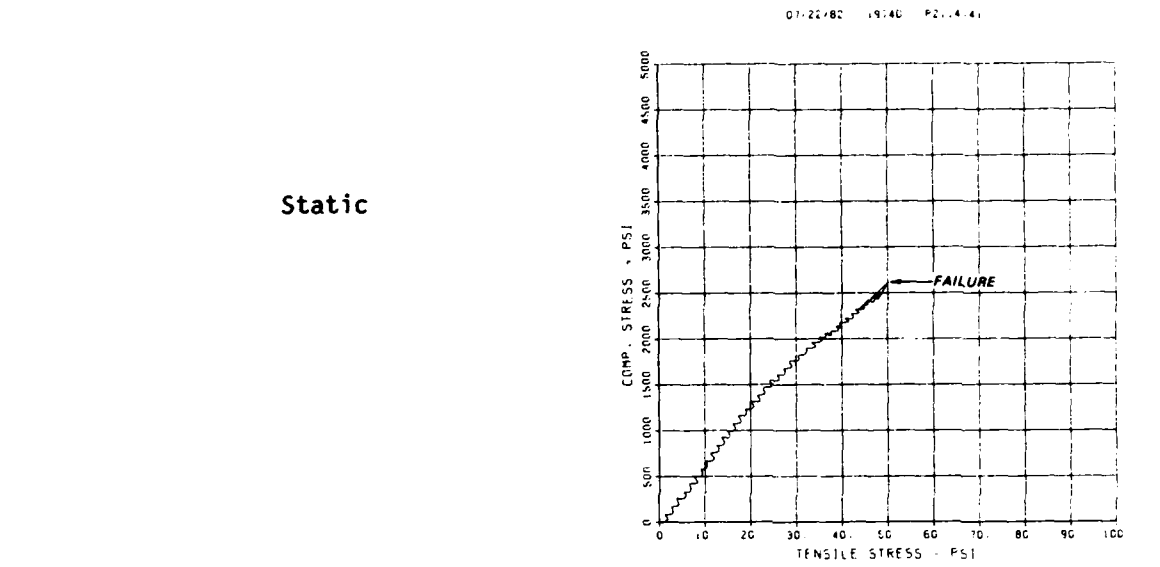

a. Dynamic load

b. Biaxial load

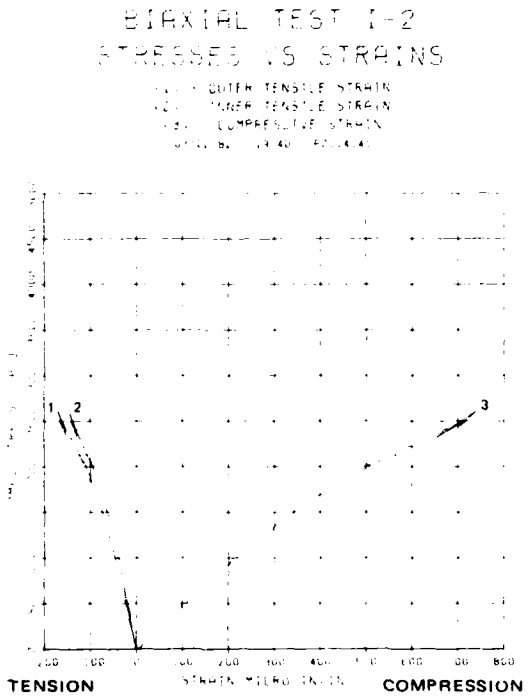

c. Strain

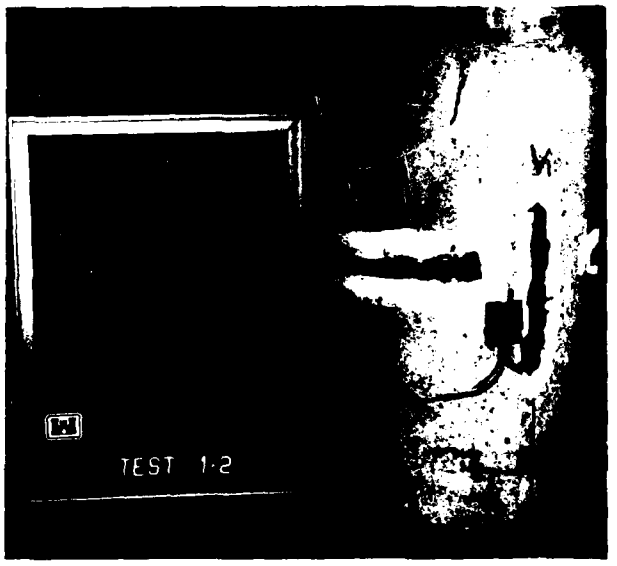

d. Failed specimen

Figure 3.2 Results of Test I-2.

Static

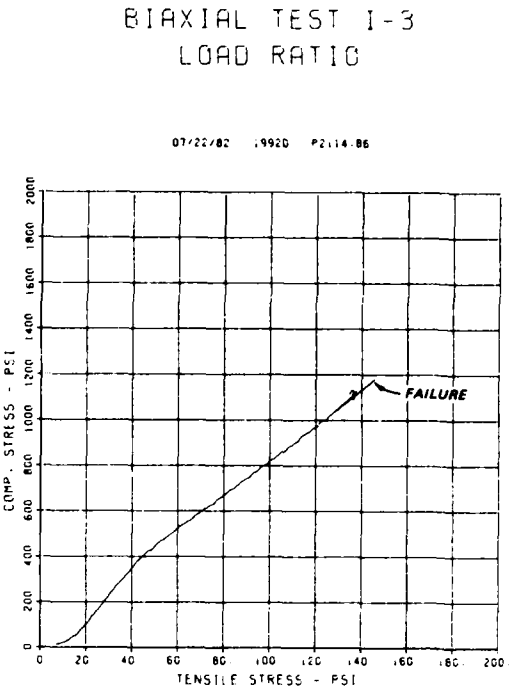

a. Dynamic load

b. Biaxial load

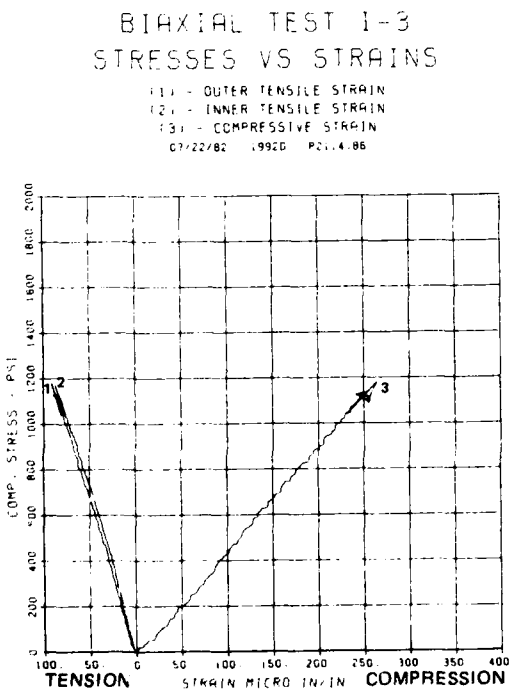

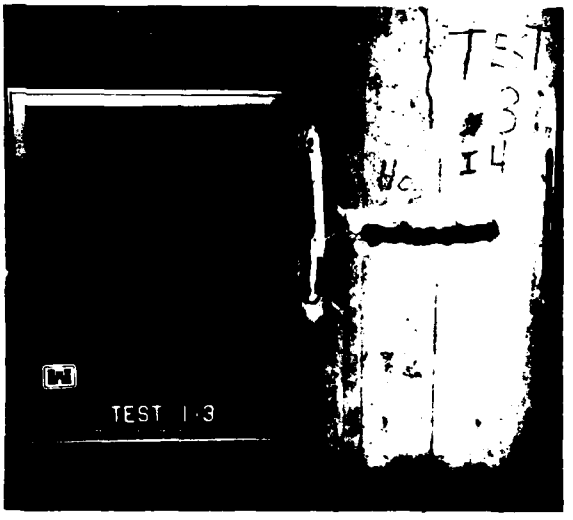

c. Strain

d. Failed specimen

Figure 3.3 Results of Test I-3.

Static

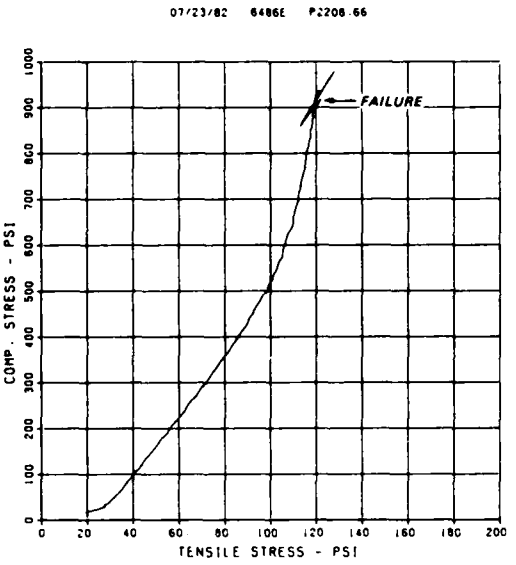

a. Dynamic load

b. Biaxial load

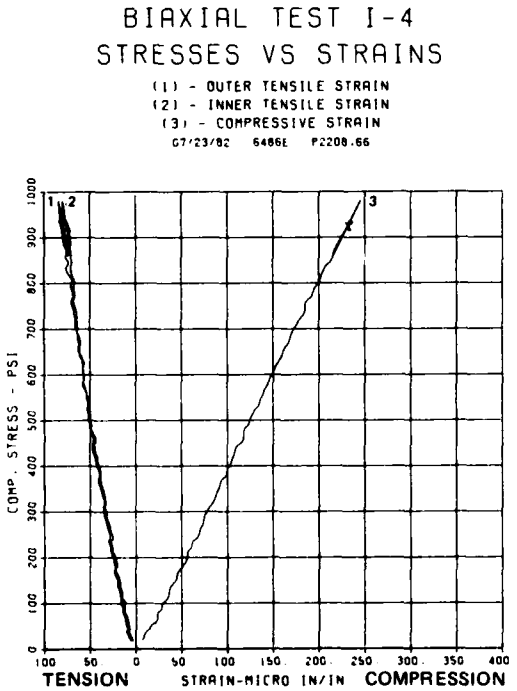

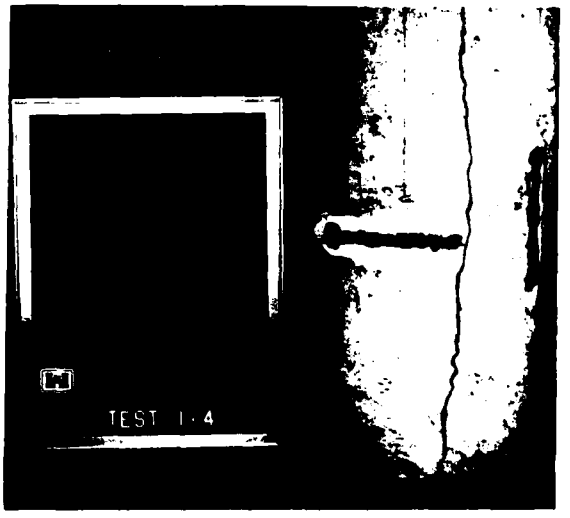

c. Strain

d. Failed specimen

Figure 3.4 Results of Test I-4.

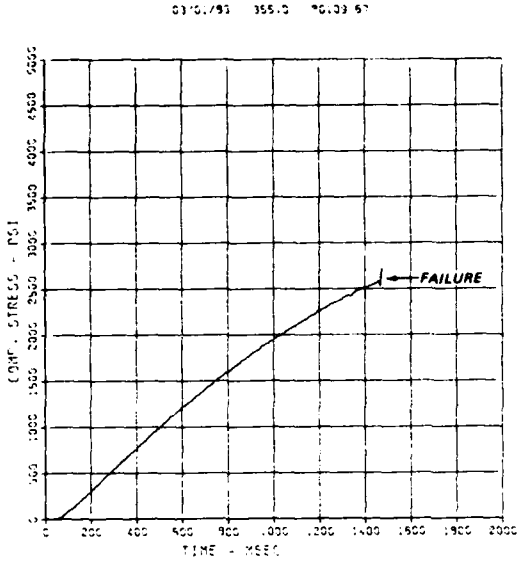

a. Dynamic load

Uniaxial

b. Biaxial load

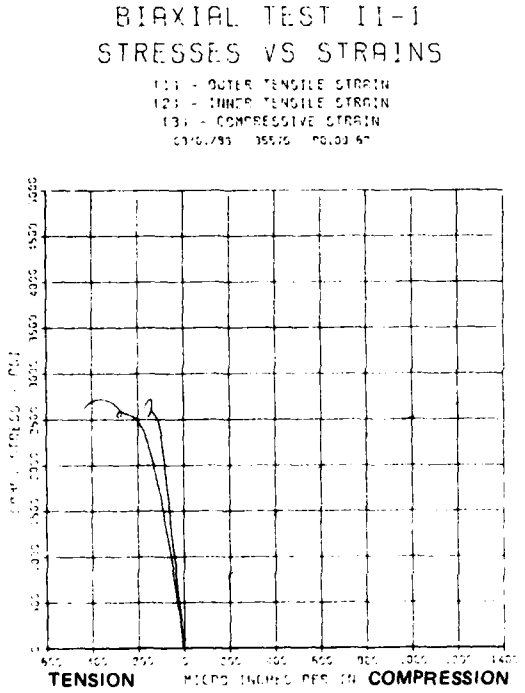

c. Strain

Disintegrated

d. Failed specimen

Figure 3.5 Results of Test II-1.

BIAXIAL TEST II-2
LOAD HISTORY

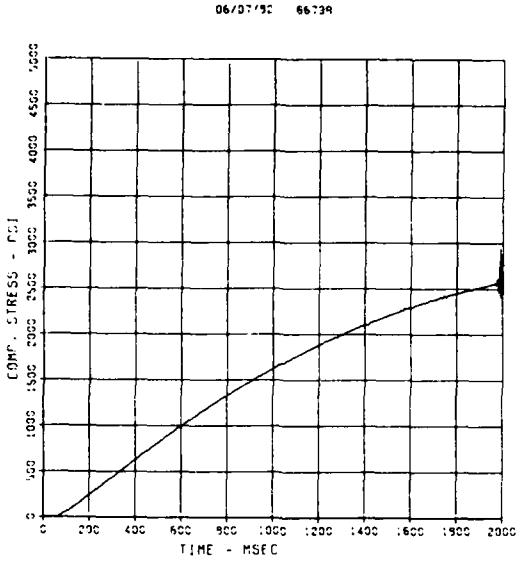

a. Dynamic load

BIAXIAL TEST II-2
LOAD RATIO

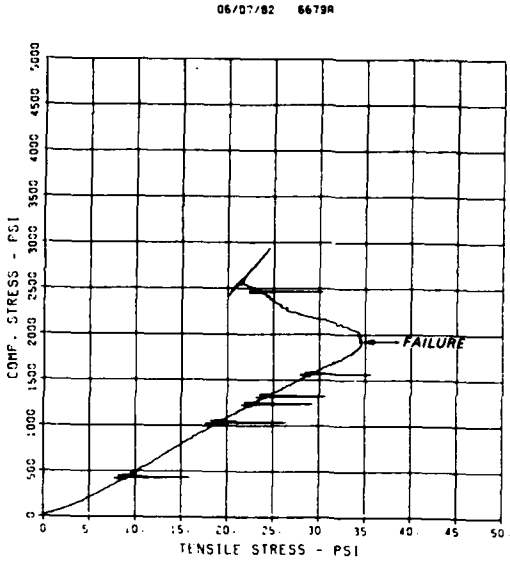

b. Biaxial load

BIAXIAL TEST II-2
STRESS VS STRAIN
(1) - OUTER TENSILE STRAIN
(2) - INNER TENSILE STRAIN
(3) - COMPRESSIVE STRAIN

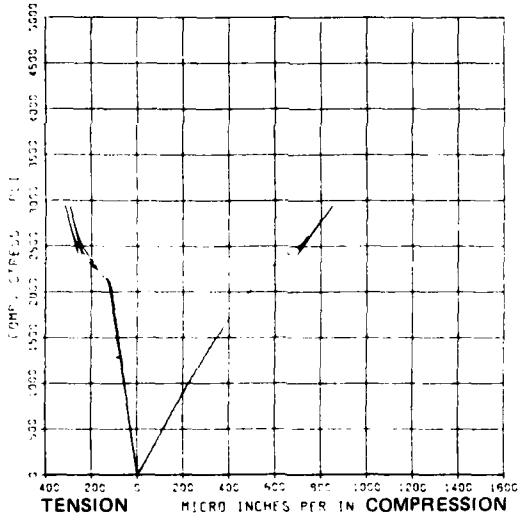

c. Strain

Disintegrated

d. Failed specimen

Figure 3.6 Results of Test II-2.

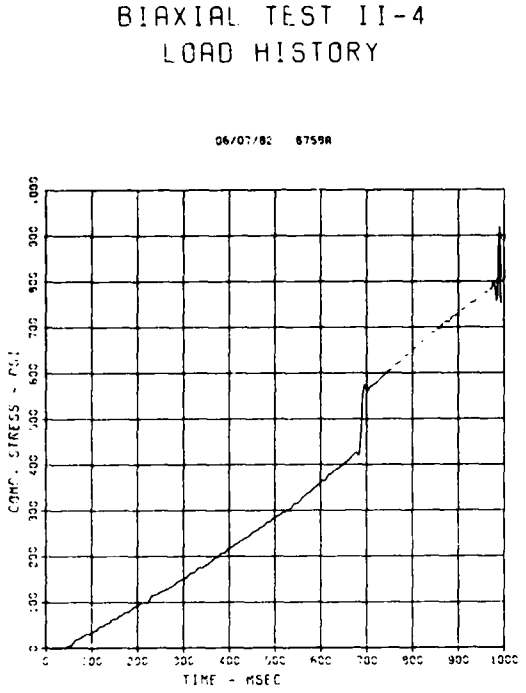

a. Dynamic load

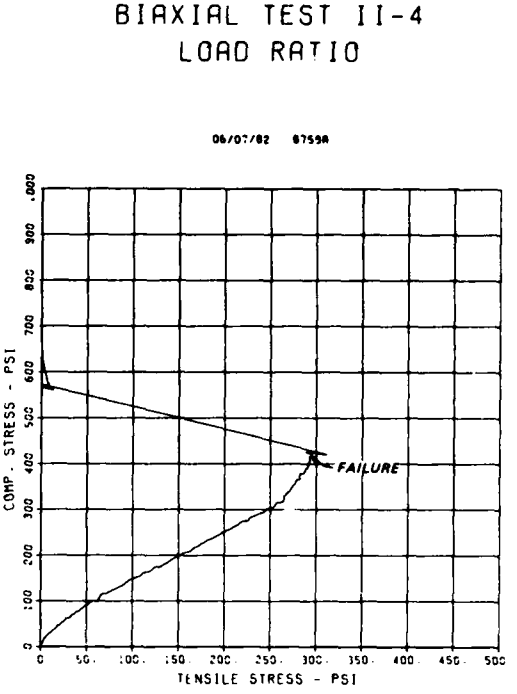

b. Biaxial load

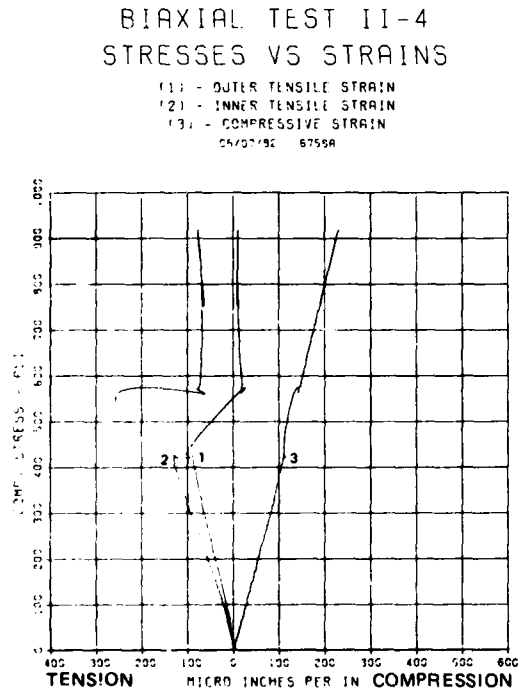

c. Strain

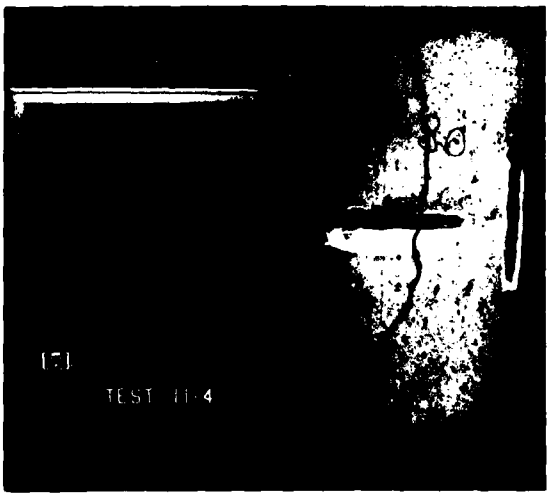

d. Failed specimen

Figure 3.7 Results of Test II-4.

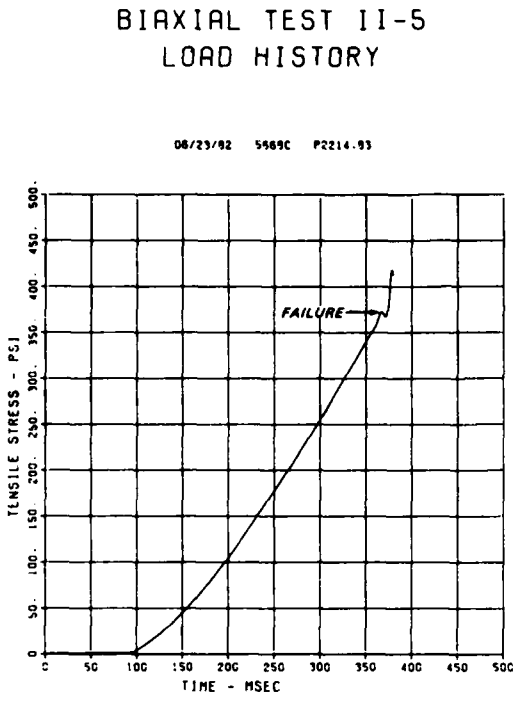

a. Dynamic load

Uniaxial

b. Biaxial load

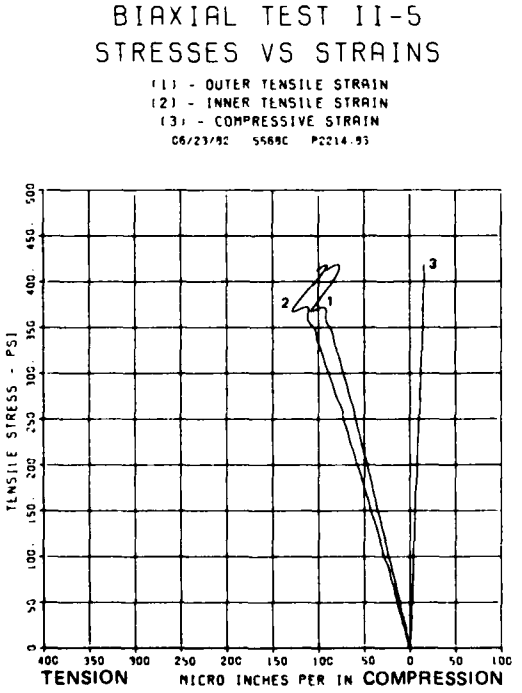

c. Strain

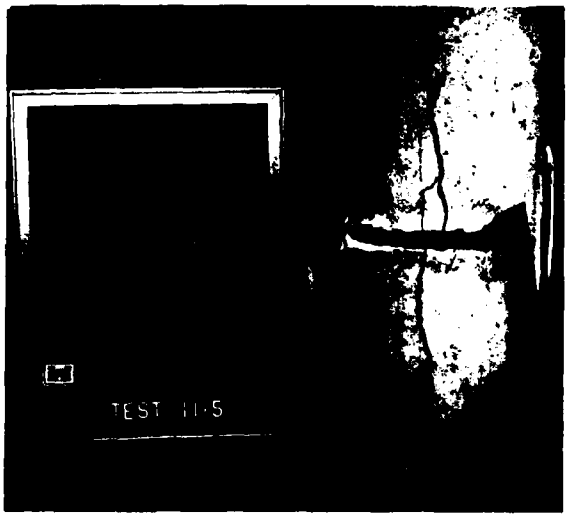

d. Failed specimen

Figure 3.8 Results of Test II-5.

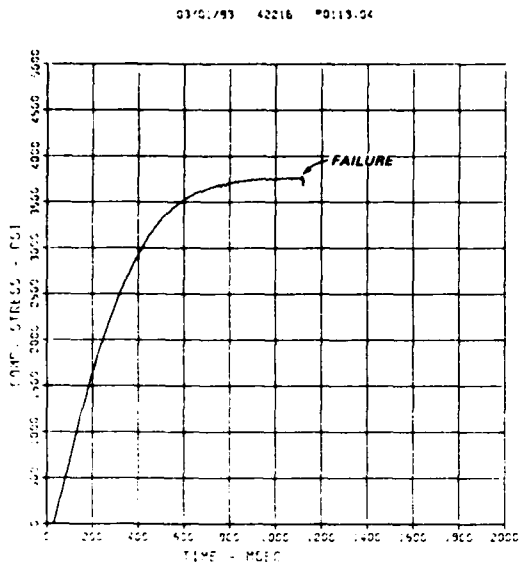

a. Dynamic load

Uniaxial

b. Biaxial load

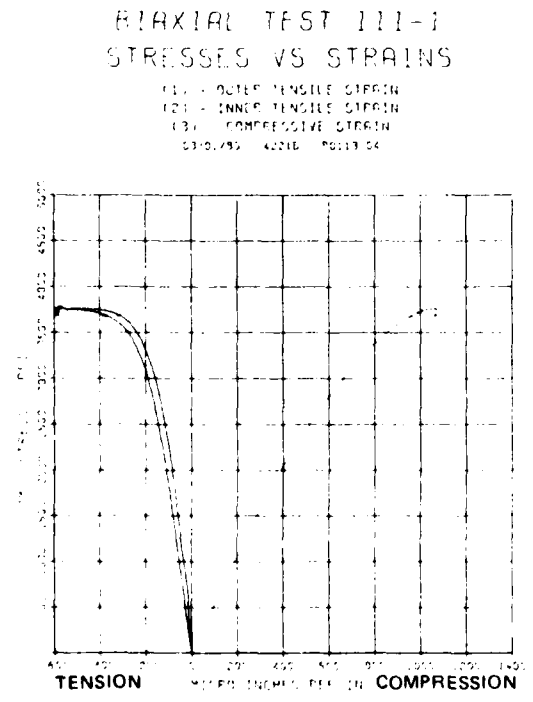

c. Strain

Disintegrated

d. Failed specimen

Figure 3.9 Results of Test III-1.

BIAXIAL TEST III-2A
LOAD HISTORY

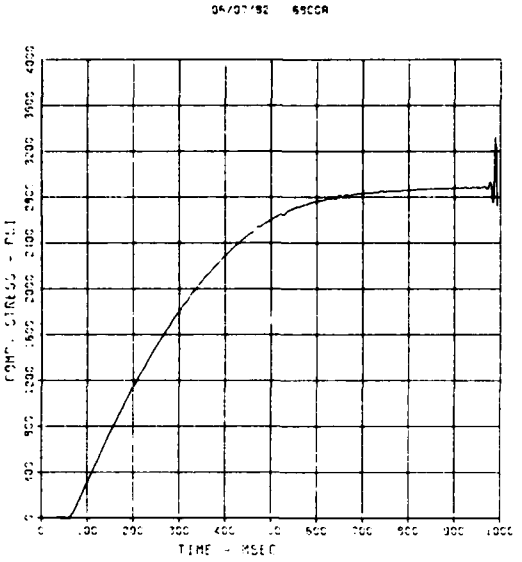

a. Dynamic load

BIAXIAL TEST III-2A
LOAD RATIO

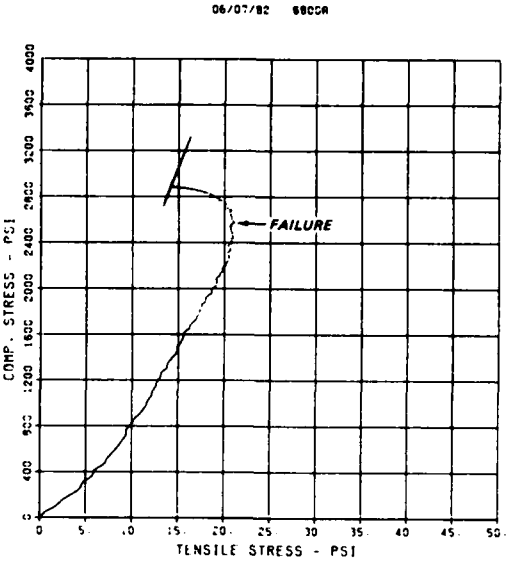

b. Biaxial load

BIAXIAL TEST III-2A
STRESSES VS STRAINS
(1) - OUTER TENSILE STRAIN
(2) - INNER TENSILE STRAIN
(3) - COMPRESSIVE STRAIN

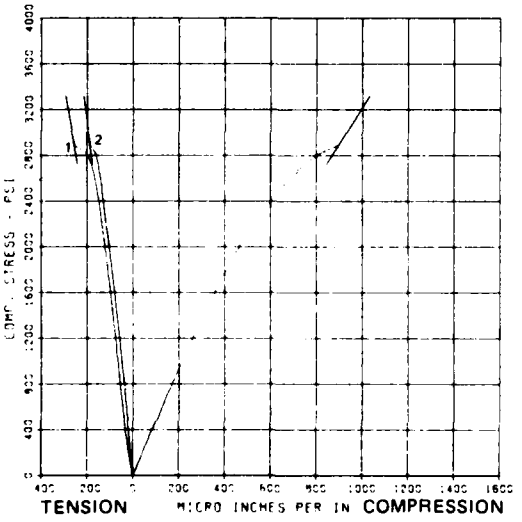

c. Strain

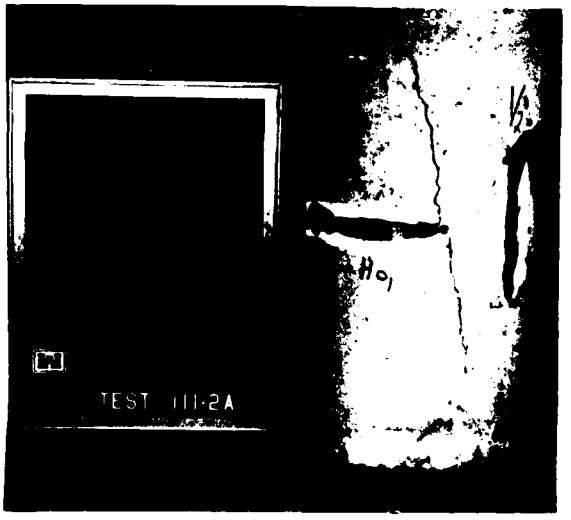

d. Failed specimen

Figure 3.10 Results of Test III-2A.

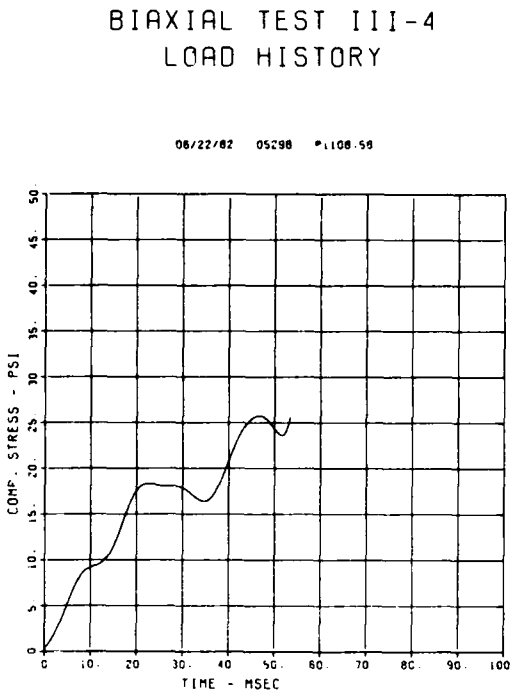

a. Dynamic load

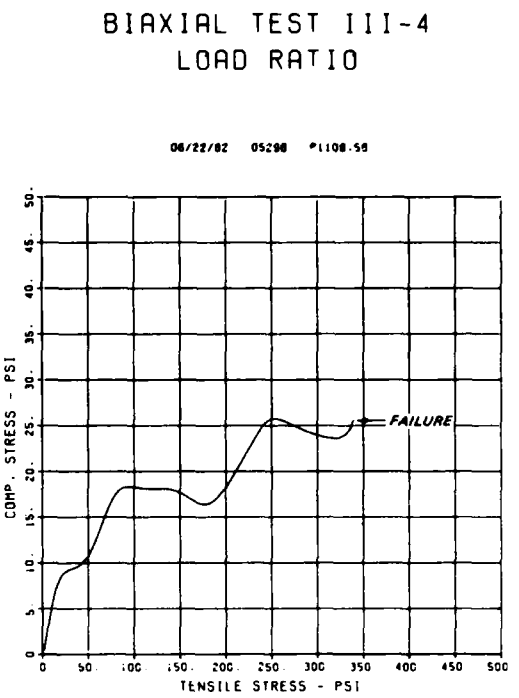

b. Biaxial load

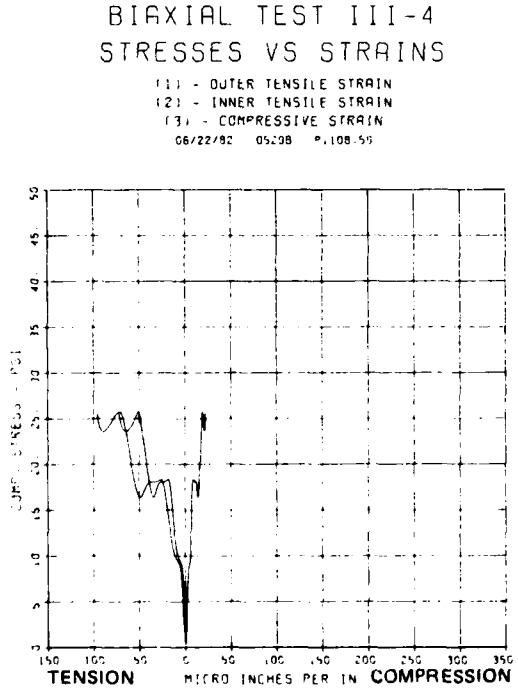

c. Strain

d. Failed specimen

Figure 3.11 Results of Test III-4.

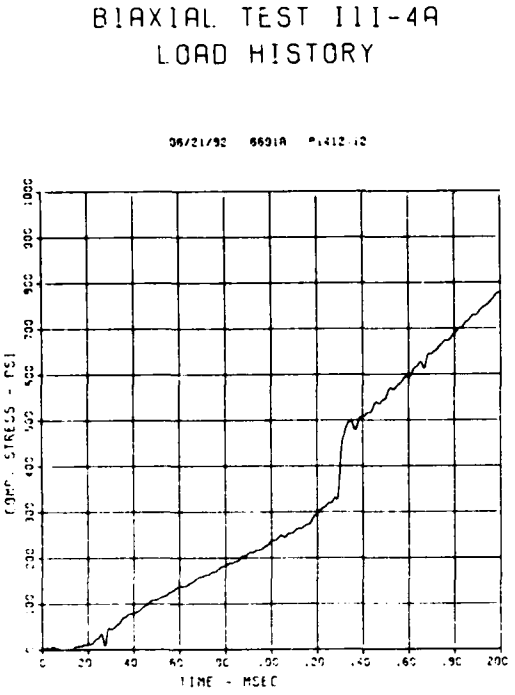

a. Dynamic load

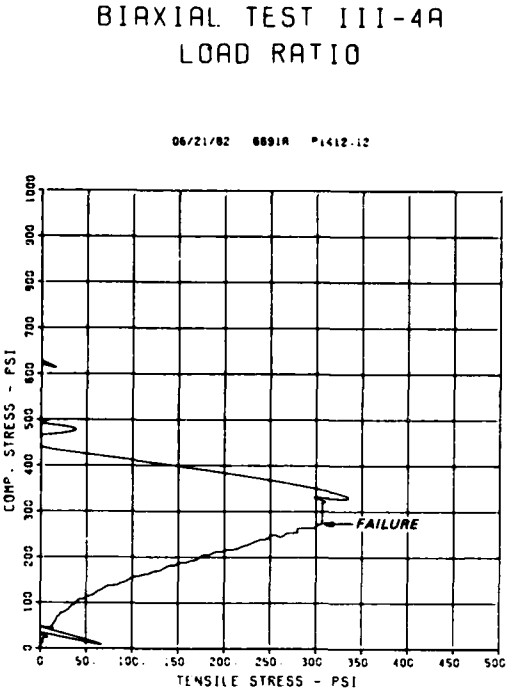

b. Biaxial load

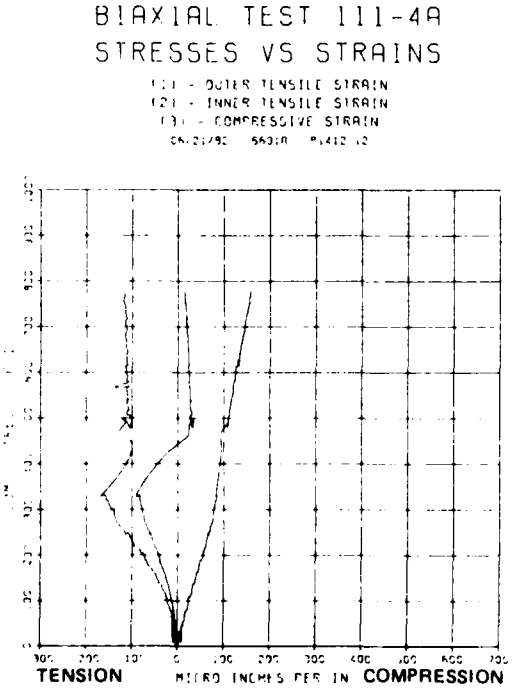

c. Strain

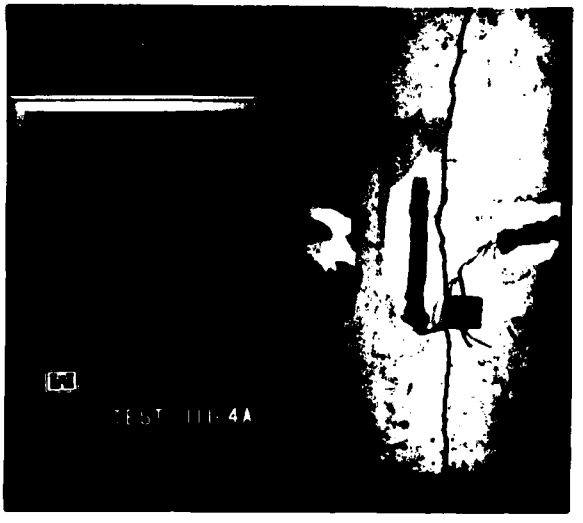

d. Failed specimen

Figure 3.12 Results of Test III-4A.

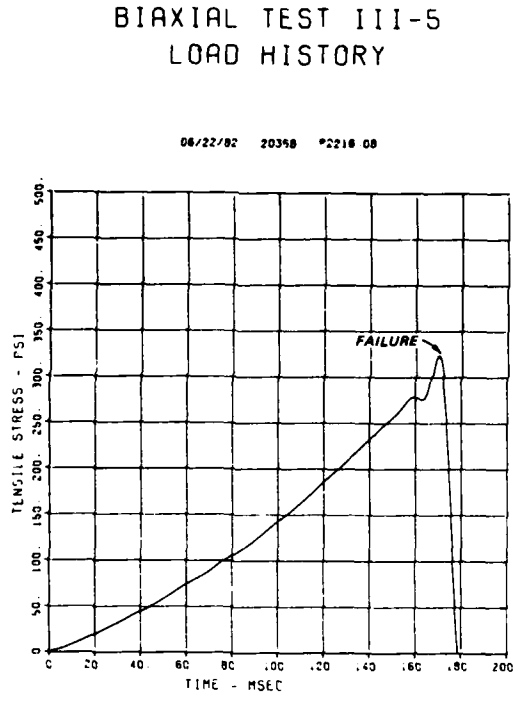

a. Dynamic load

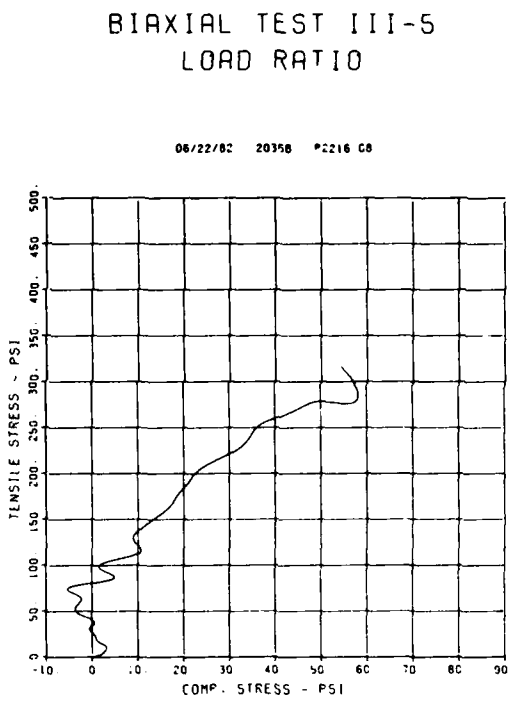

b. Biaxial load

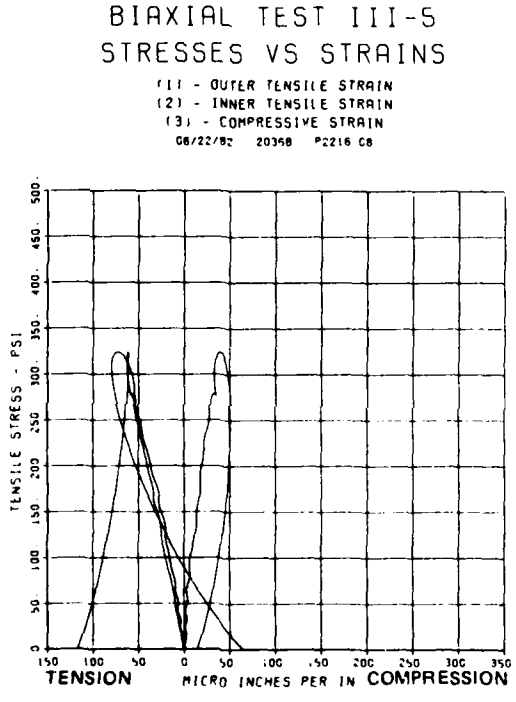

c. Strain

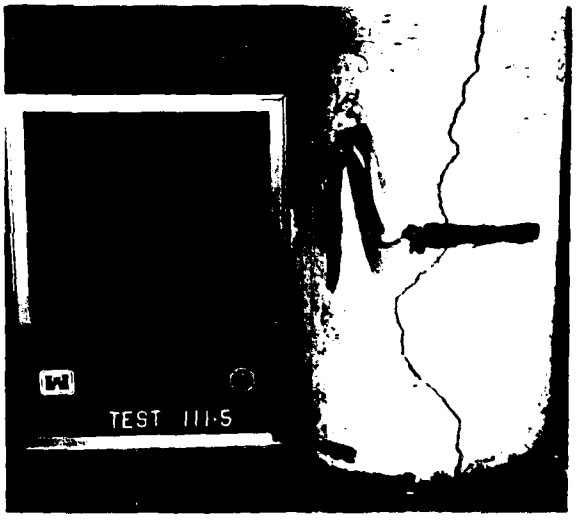

d. Failed specimen

Figure 3.13 Results of Test III-5.

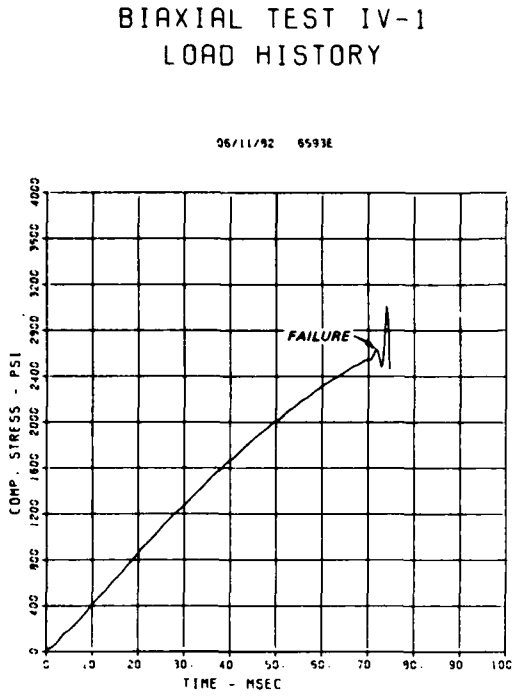

a. Dynamic load

Uniaxial

b. Biaxial load

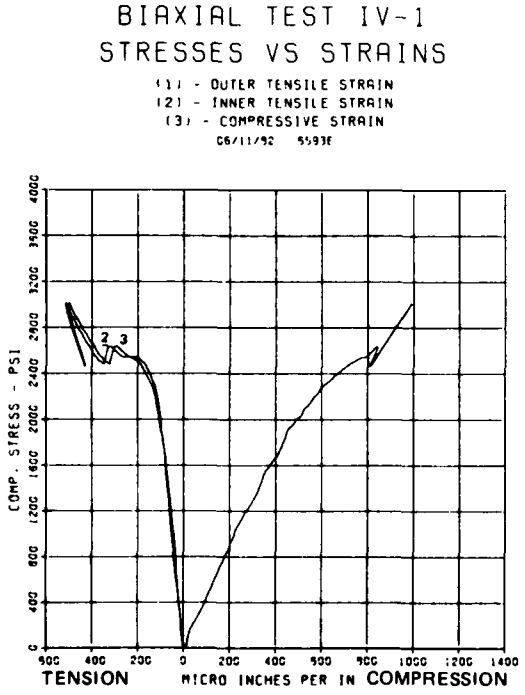

c. Strain

Disintegrated

d. Failed specimen

Figure 3.14 Results of Test IV-1.

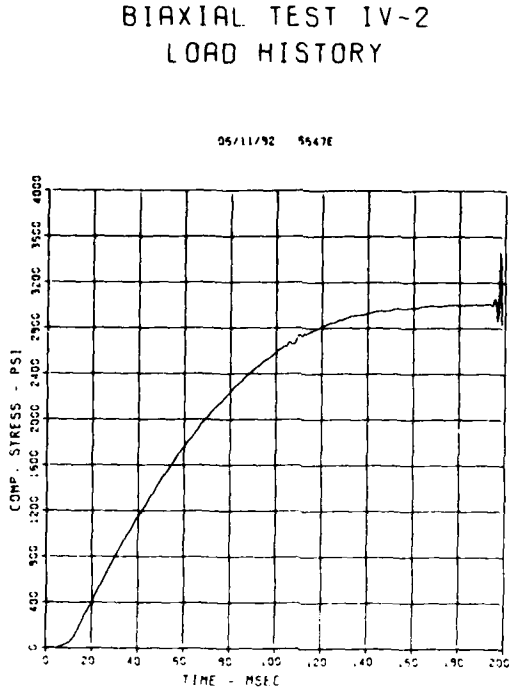

a. Dynamic load

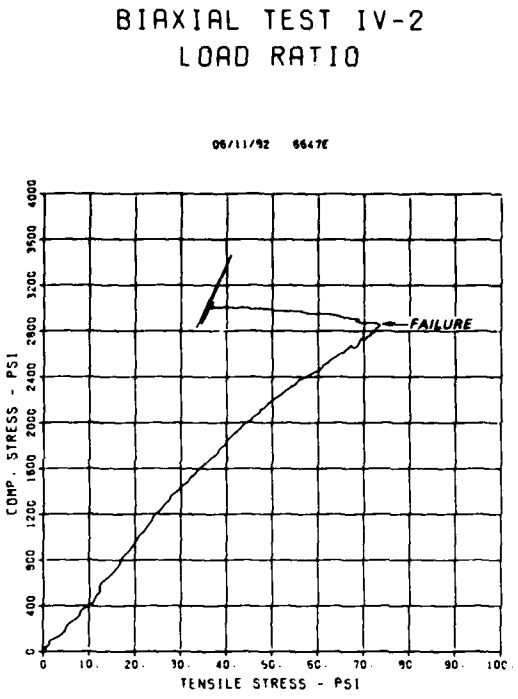

b. Biaxial load

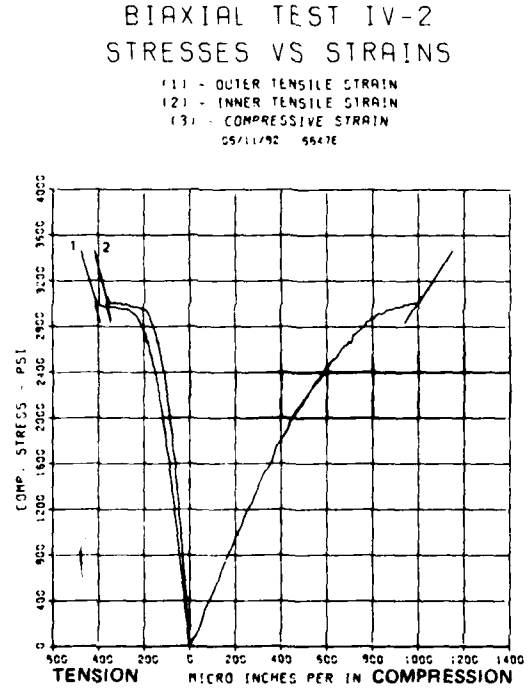

c. Strain

Disintegrated

d. Failed specimen

Figure 3.15 Results of Test IV-2.

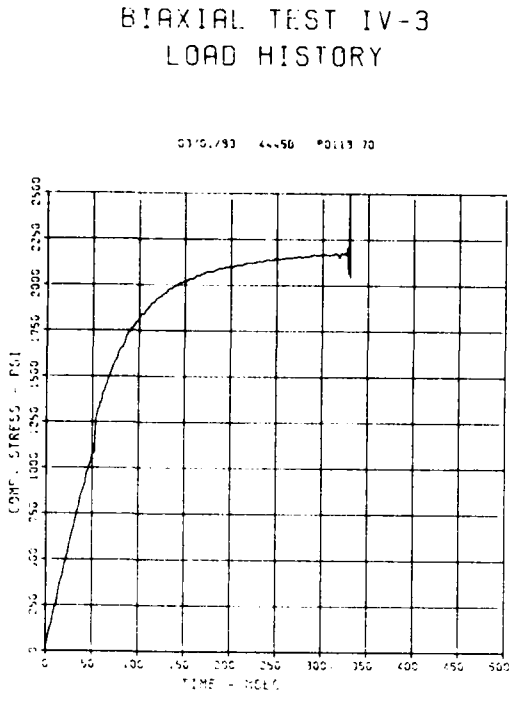

a. Dynamic load

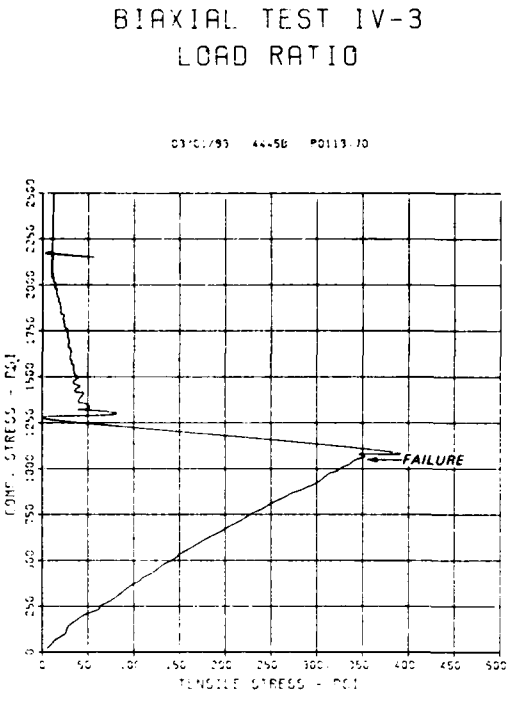

b. Biaxial load

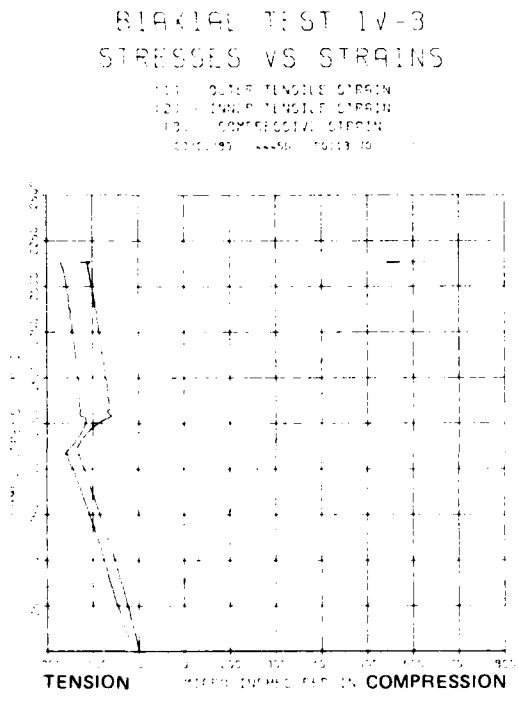

c. Strain

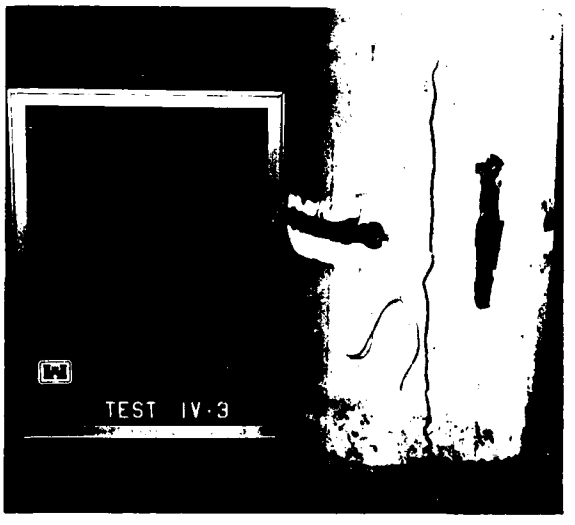

d. Failed specimen

Figure 3.16 Results of Test IV-3.

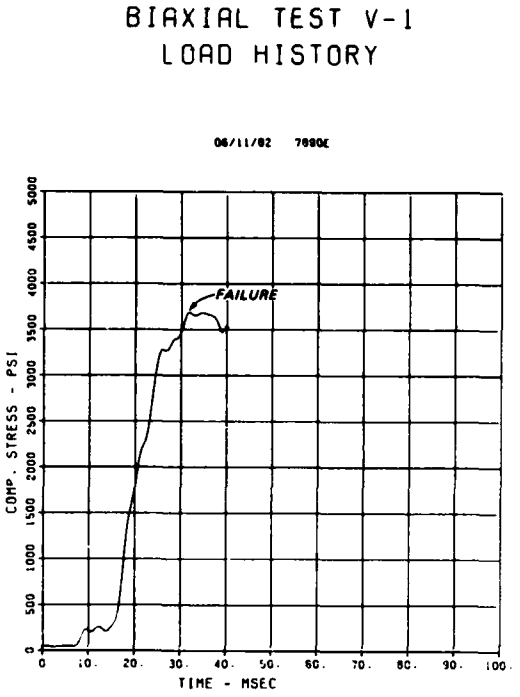

a. Dynamic load

Uniaxial

b. Biaxial load

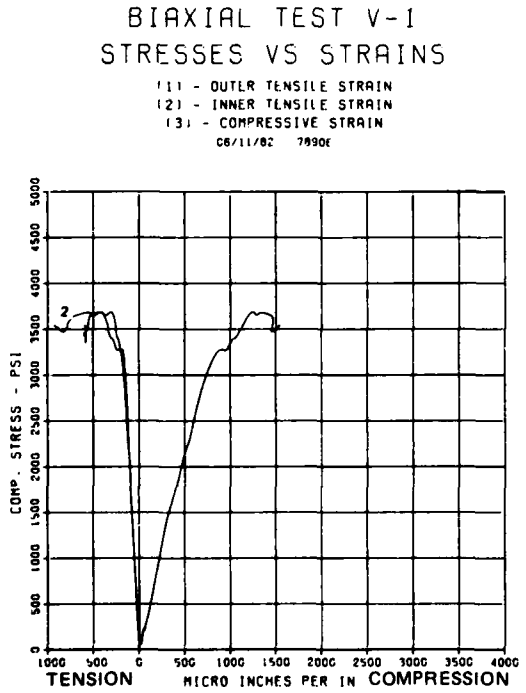

c. Strain

Disintegrated

d. Failed specimen

Figure 3.17 Results of Test V-1.

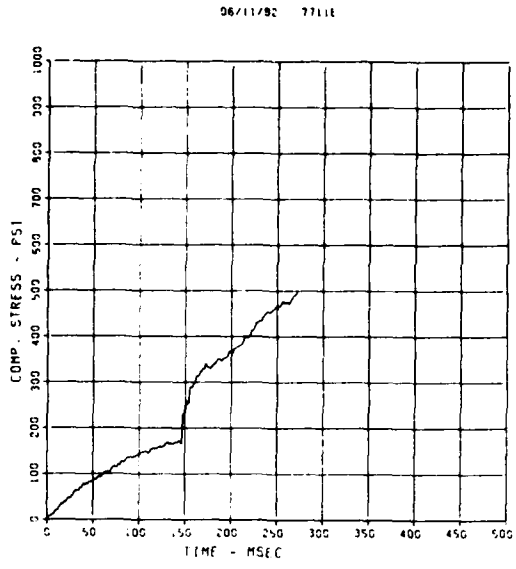

a. Dynamic load

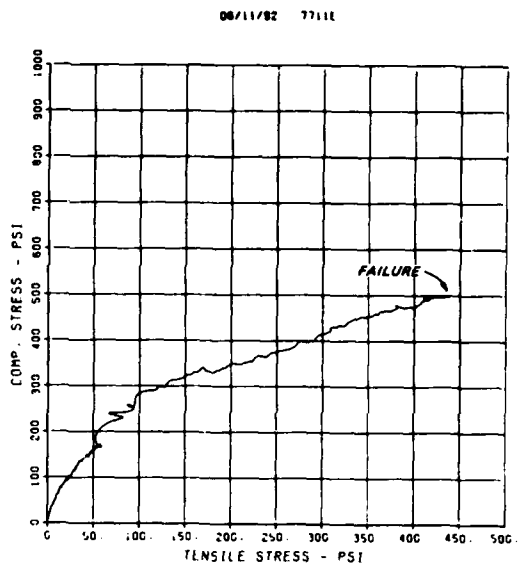

b. Biaxial load

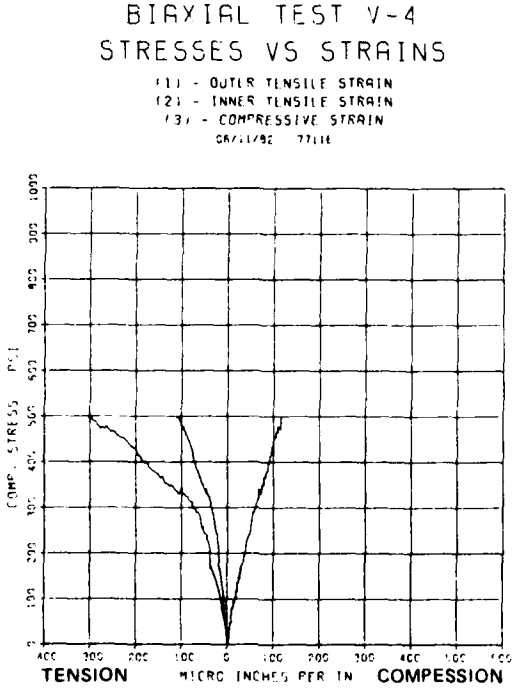

c. Strain

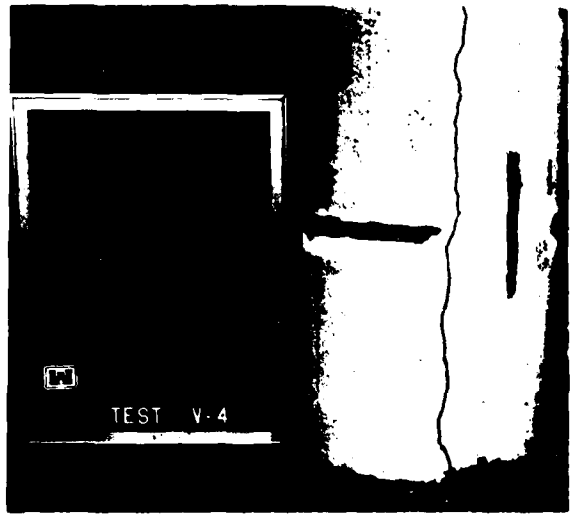

d. Failed specimen

Figure 3.18 Results of Test V-4.

CHAPTER 4

DISCUSSION

4.1 CONTROL CYLINDERS

The distribution of control cylinder compressive strength, by lot, is shown in Figure 4.1. The 3333-psi grand mean is 11 percent above the nominally desired 90-day strength. It is noted that lots a-d appear stronger than e-h for no plausible reason. The 7 percent coefficient of variation (COV) indicates that reasonable uniform quality was attained among lots. Nonetheless, the control cylinder tensile strengths (in Figure 4.2) have a grand mean which is a plausible 9 percent of the average compressive strength. Notice the 16 percent COV for tensile strength, which suggests this parameter is more variable than the compressive strength. The distributions of strain-at-failure appear in Figures 4.3 through 4.5. It appears that failure strains vary more under identical conditions than do failure stresses.

4.2 FAILURE MODES

The failure modes of the dynamic specimens are shown as a function of their biaxial-stress state in Figure 4.6. Those specimens loaded in uniaxial compression disintegrated completely and explosively under the dynamic loading. On the other hand, single longitudinal cleavage failures occurred in those specimens loaded significantly in tension. The transition from compressive failure to tensile failure is rapid as the percent of tension increases. These observations are consistent with those of the static tests by McHenry and Karni (1958) and Kupfer, Hilsdorf, and Rusch (1969).

4.3 STRENGTH DATA

To interpret the dynamic, biaxial strength results in Table 3.2, a stepwise statistical-regression procedure was conducted, as described in Draper and Smith (1966). The form of this regression equation was taken to be linear between σ_c and σ_t for constant t_r, which approximates the accepted static, tension-compression behavior in Figure 1.1. The form of the equation was also assumed to be linear with respect to $\ell n\ t_r$ for a constant σ_c/σ_t ratio which agrees with previous uniaxial, dynamic findings in Figure 1.2. The result of the regression analysis, shown in Figure 4.7, is

$$\frac{\sigma_c}{\sigma_{cs}} + \frac{\sigma_t}{\sigma_{ts}} = 1 - 0.02503 \ln \frac{t_r}{t_s} \pm s_\sigma \quad , \qquad \begin{matrix} t_s < t_r < 25 \text{ ms} \\ \sigma_c \geq 0 \ , \ \sigma_t \geq 0 \end{matrix} \qquad (1)$$

in which

σ_c = compressive stress at failure

σ_{cs} = estimated static uniaxial compressive strength = 2520 psi

σ_t = tensile stress at failure

σ_{ts} = estimated static uniaxial tensile strength = 325 psi

t_r = time since load application at which failure occurs

t_s = time of static load application = 600,000 ms

s_σ = standard error of estimate = 0.2321

The square of the regression's multiple correlation coefficient, $r^2 = 0.8254$, indicates that all but 17 percent of the strength variability in Table 3.2 is explained by this equation. In light of control cylinder strength variability in tension, much of this residual variability may represent material differences in the concrete. Neither σ_{cs} nor σ_{ts} agrees identically with the corresponding measured uniaxial static strength. This is of no particular significance, since these estimates were selected to fit all the biaxial dynamic measurements.

In Figure 4.8, the biaxial aspect of the regression is compared with the dynamic data, previous static theory, and the control cylinders. Note that the strength axes in this figure have been factored by the dynamic effect of the regression equation, $1 - 0.02503 \ln t_r/t_s$. This removal of dynamic dependence causes the data to scatter less than in the unfactored plot of Figure 4.6. The factoring also reduces the regression equation from the family of lines shown in Figure 4.7 to a single line centered in the data. To within the data's accuracy, the results are seen to be consistent with a static theory previously shown in Figure 1.1 to represent existing static data. Also, to within the dynamic data's scatter, the regression's estimated uniaxial stengths are in agreement with the control-cylinder results.

Figure 4.9 illustrates the dynamic side of the regression result. The ordinate of this graph measures the biaxial strength in the form assumed by the regression. In spite of the dynamic data scatter, there is seen to be some logarithmic dependence of biaxial strength on the loading time t_r which is explained by the regression equation. This behavior agrees with previous

uniaxial, dynamic results to the extent shown. The dynamic results are consistent with the control cylinder tests as well.

Practically speaking, the regression equation 1 and Figure 4.7 indicate that the biaxial strength increases significantly under dynamic loading. For example, a gravity dam with a fundamental period of 0.2 second would have its loading applied during an earthquake in approximately $t_r = 0.2 \text{ sec}/4 = 50 \text{ ms}$. If the structure's concrete material were similar to that studied therein, one could expect biaxial strengths from equation 1 that are about 24 percent greater than static values. However, this increase should be used cautiously as the standard error of this estimate is 23 percent.

4.4 STRAIN DATA

A stepwise-regression analysis was also performed on the strains-at-failure given in Table 3.2. The result illustrated in Figure 4.10 is

$$\frac{\varepsilon_c}{\varepsilon_{cs}} - \frac{\varepsilon_t}{\varepsilon_{ts}} = 1 \pm s_\varepsilon \quad , \quad \begin{array}{l} t_s < t_r < 25 \text{ ms} \\ \varepsilon_c > 15 \text{ μin/in} \\ \varepsilon_t > 60 \text{ μin/in} \end{array} \qquad (2)$$

in which

ε_c = compressive strain at failure
ε_{cs} = estimated uniaxial compressive strain = 11.68 μin/in
ε_t = tensile strain at failure
ε_{ts} = estimated uniaxial tensile strain = 4.25 μin/in
s_ε = standard error of estimate = 25.17
t_s = time of static load application = 600,000 ms
t_r = time since load application at which failure occurs

This equation explains $r^2 = 0.6314$ of the strain variability in Table 3.2. That there is more residual variation of strain than there is of strength is not unexpected since the strain distribution of the control cylinders varied more than their strength distributions also. The estimated ε_{cs} and ε_{ts} refer to hypothetical uniaxial strain loadings and thus should not be compared to the strains measured for uniaxial stress loadings.

The biaxial dependence of strains-at-failure is shown in Figure 4.11. The dynamic data are seen to follow the trend of equation 2. Note that they are consistent with strains-at-static failure taken from Kupfer, Hilsdorf, and

Rusch (1969), as well. Although smaller in magnitude, the dynamic strains-at-failure are also seen to be in approximately the same ratio as the static control data.

The independence of biaxial strain on dynamic loading, implied by equation 2, is shown in Figure 4.12. There is seen to be no significant dependence of the biaxial strain measured by the form of equation 2 upon the loading time t_r . The static control cylinder tests also agree with this result. This independence of strain and loading time has been previously noted under uniaxial conditions (as in Figure 1.2).

A useful implication of these strain results is that failure under dynamic, biaxial loadings might be judged by a strain criterion rather than a strength criterion. An advantage of the former is that the same standard would be applicable for dynamic and static loadings. However, the standard error of estimate, and hence uncertainty, of the strain criteron would be greater than that of a stress criterion.

4.5 STRESS-STRAIN BEHAVIOR

The two previous sections have established that tensile-compressive strengths increase with the loadings rapidity while the failure strains remain constant. This dynamic stiffening is inconsistent with the assumption of linearly elastic behavior used in practical design analyses. However, it resembles the response of viscoelastic models which linearly relate stress to strain rate as well as strain and which have been proposed for the uniaxial behavior of concrete by Hatano (1960), Hatano and Tsutsumi (1959), and Krillov (1977). In addition to this rate dependency, the static stress strain data reflect nonlinearities which increase in importance as the biaxial load becomes more compressive in character. A viscoplastic material model, which nonlinearly relates stress, strain, and strain rate (Bazant and Oh, 1982), may explain both of these violations of linear elasticity. It would seem prudent to recommend no improvement to the design practice of modeling stress-strain behavior as linearly elastic until this or some other theoretical model is shown to conform to this data and until the broader implications of such a model are appreciated.

4.6 FURTHER RESEARCH

This study has usefully advanced seismic design by establishing the dynamic dependence of tensile-compressive stress and strain at failure. However,

additional research is desirable to better comprehend the stress-strain behavior of concrete which is also important to the seismic analysis of dams. This project has provided data base for such research. Viscoelastic material models should now be compared to these results. Contingent on the results of this comparison, viscoplastic models may also warrant investigation. Thereafter, the behavior under other biaxial stress states and under cyclic loadings should be examined. Finally, the dependence of dynamic, biaxial behavior on the constituents of the concrete mixture remains to be determined.

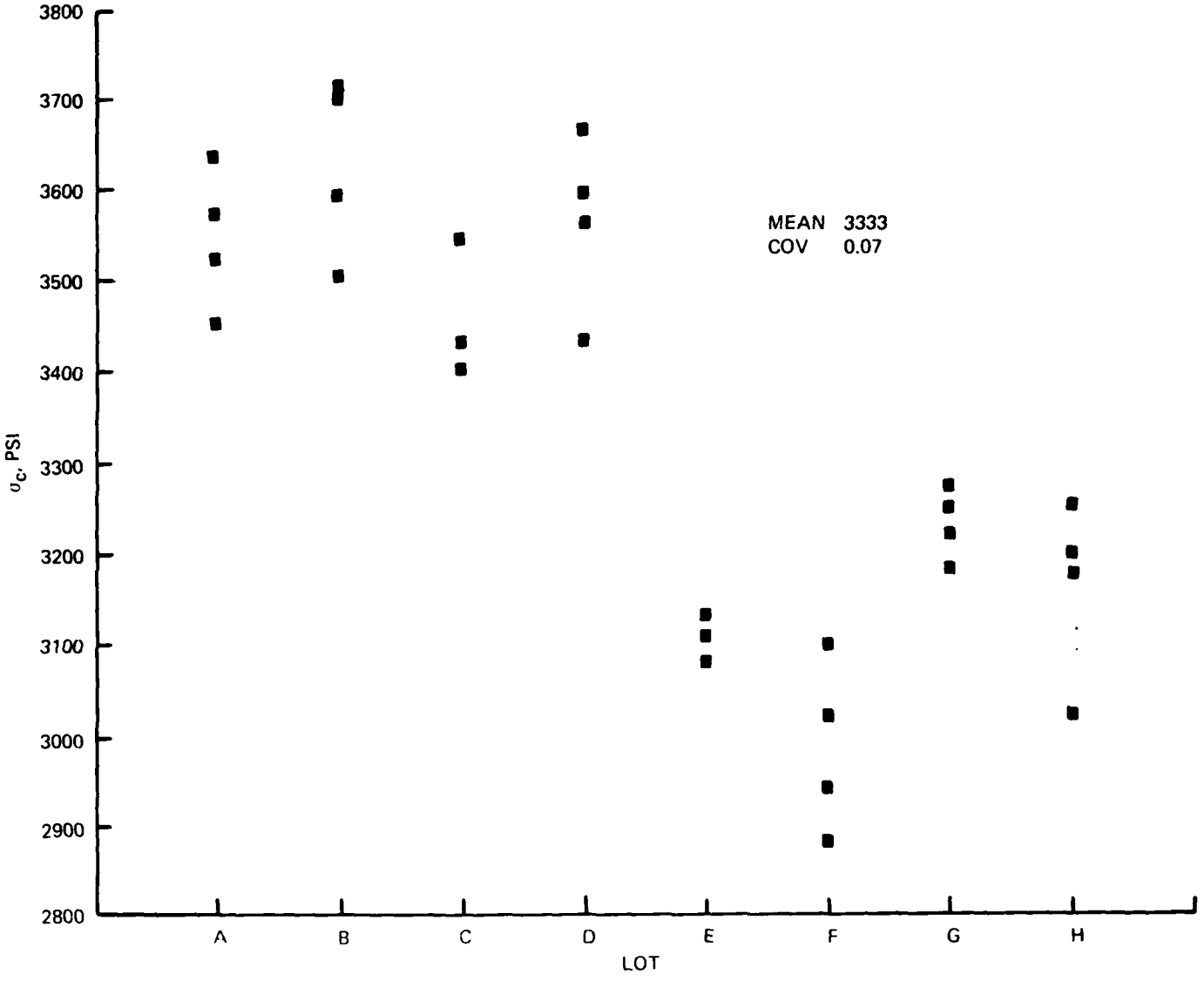

Figure 4.1 Compressive strength of control cylinders.

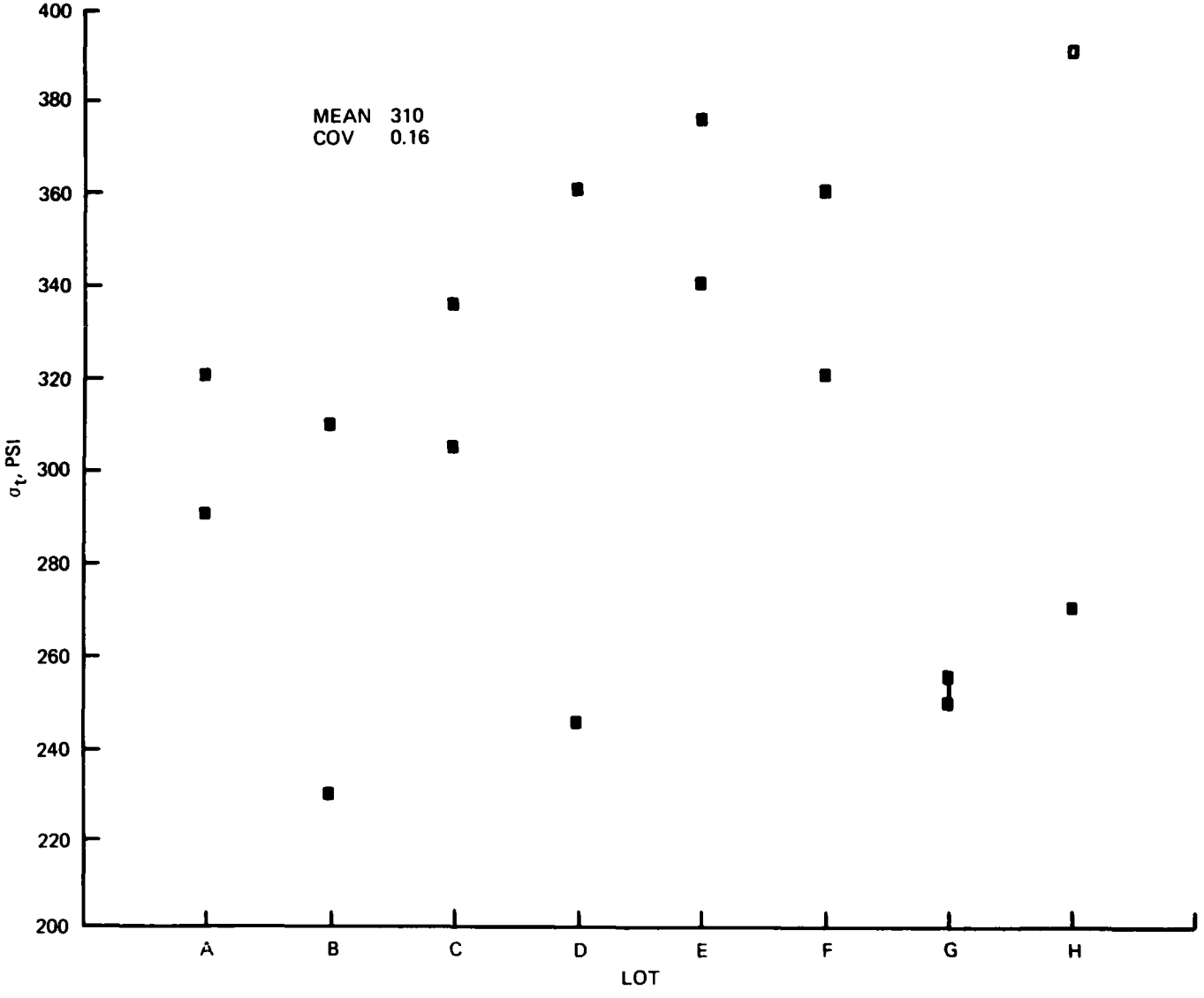

Figure 4.2 Tensile strength of control cylinders.

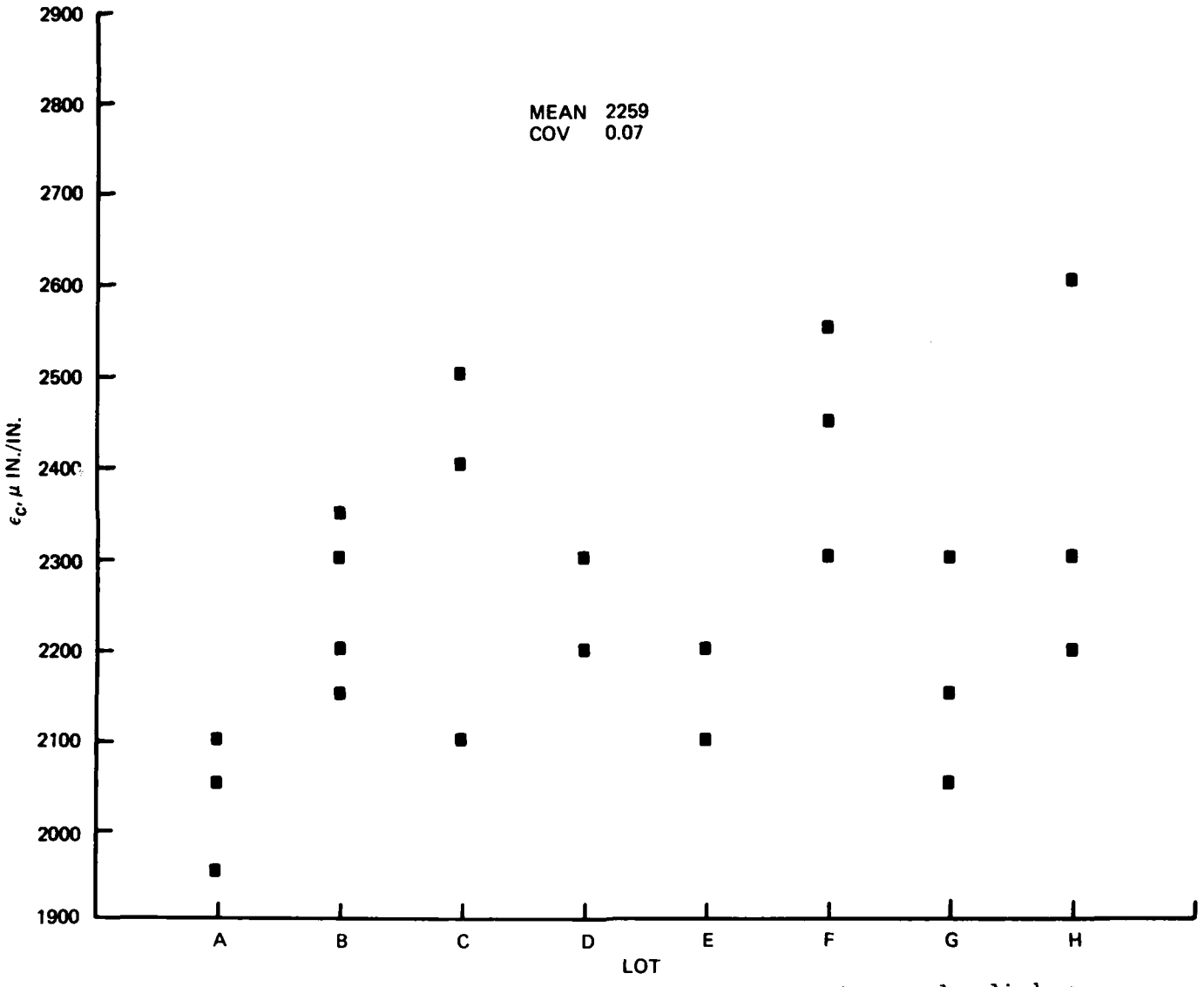

Figure 4.3 Compressive strain in uniaxial compression of control cylinders.

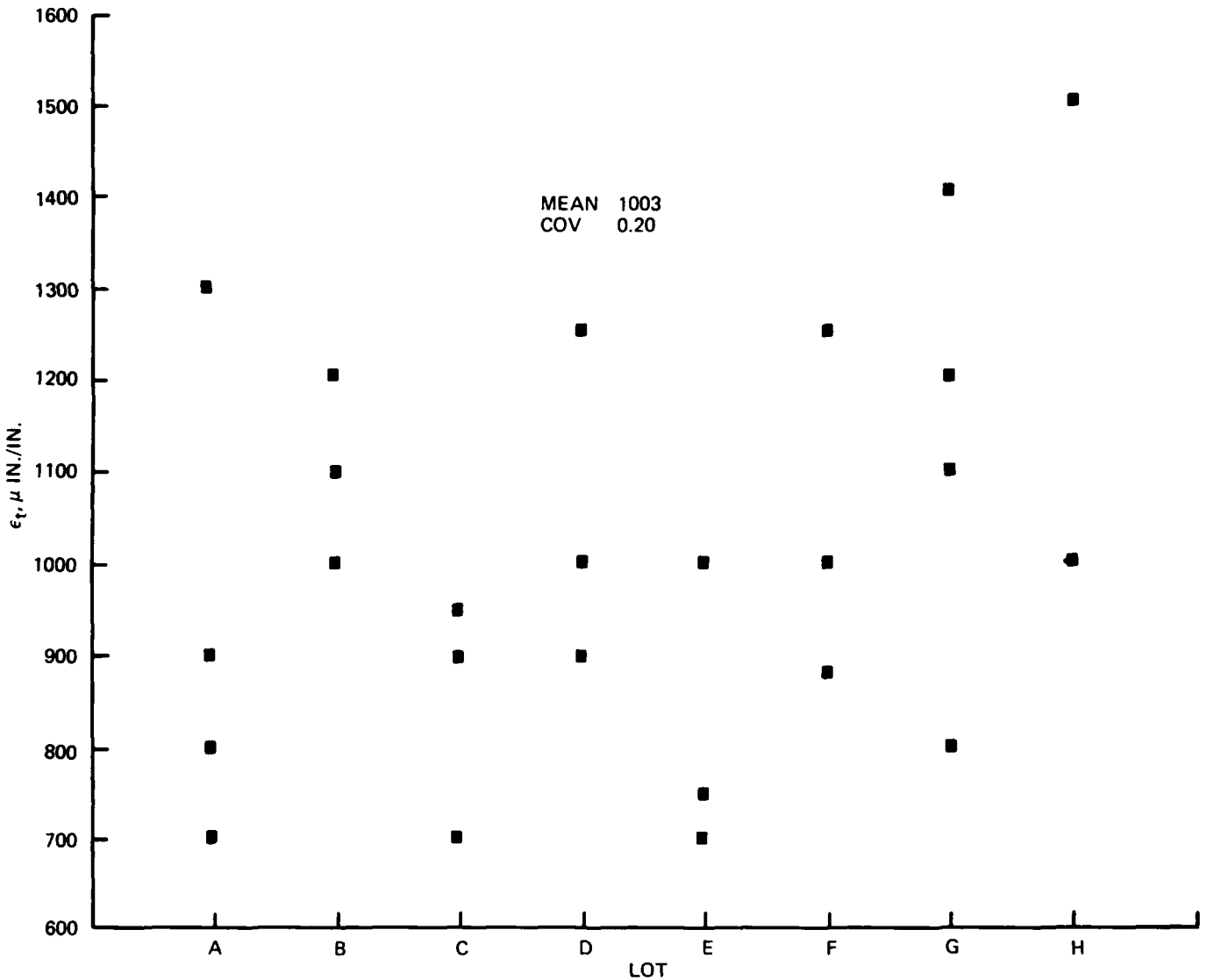

Figure 4.4 Tensile strain in uniaxial compression of control cylinders.

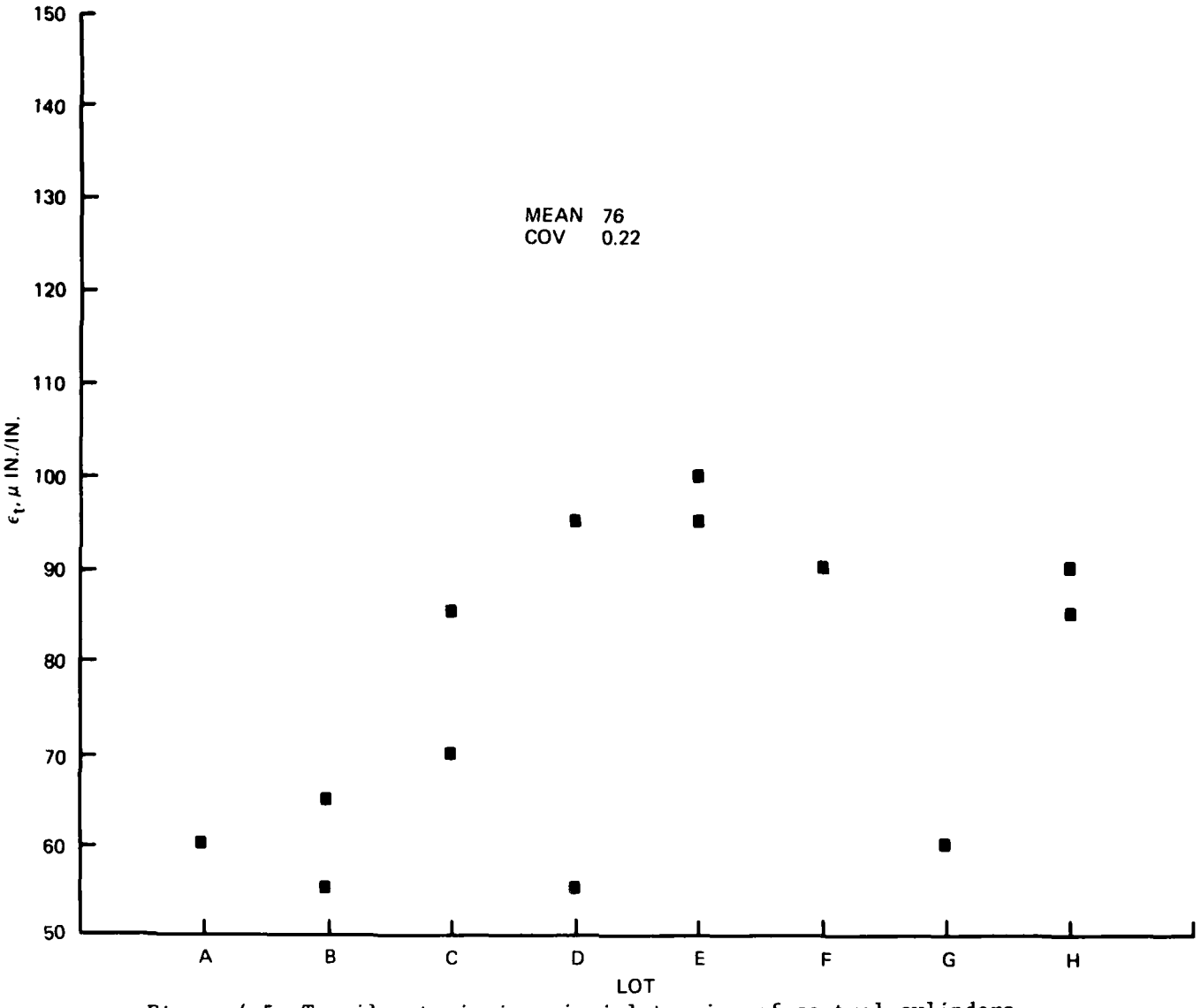

Figure 4.5 Tensile strain in uniaxial tension of control cylinders.

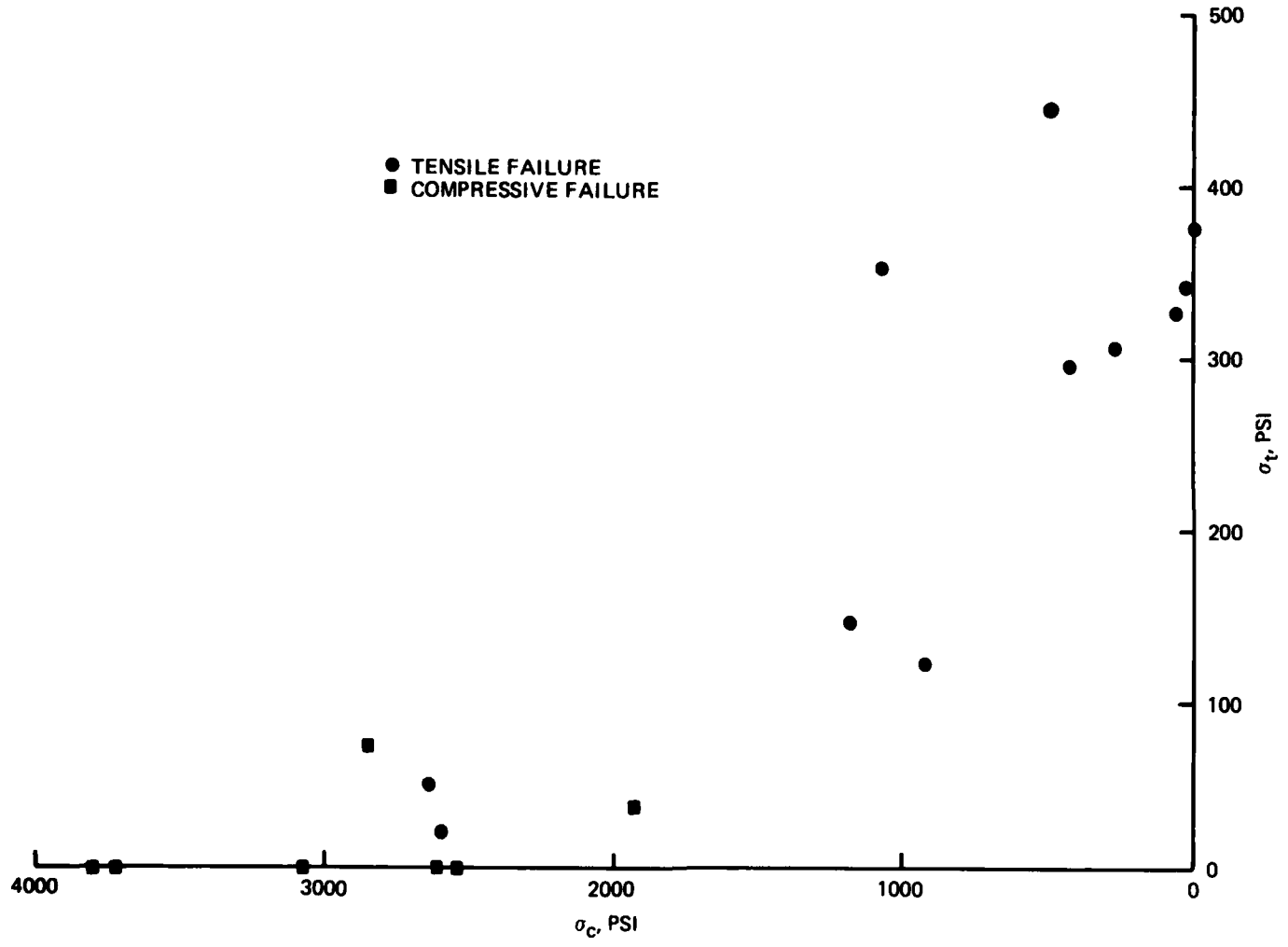

Figure 4.6 Dynamic biaxial failure modes.

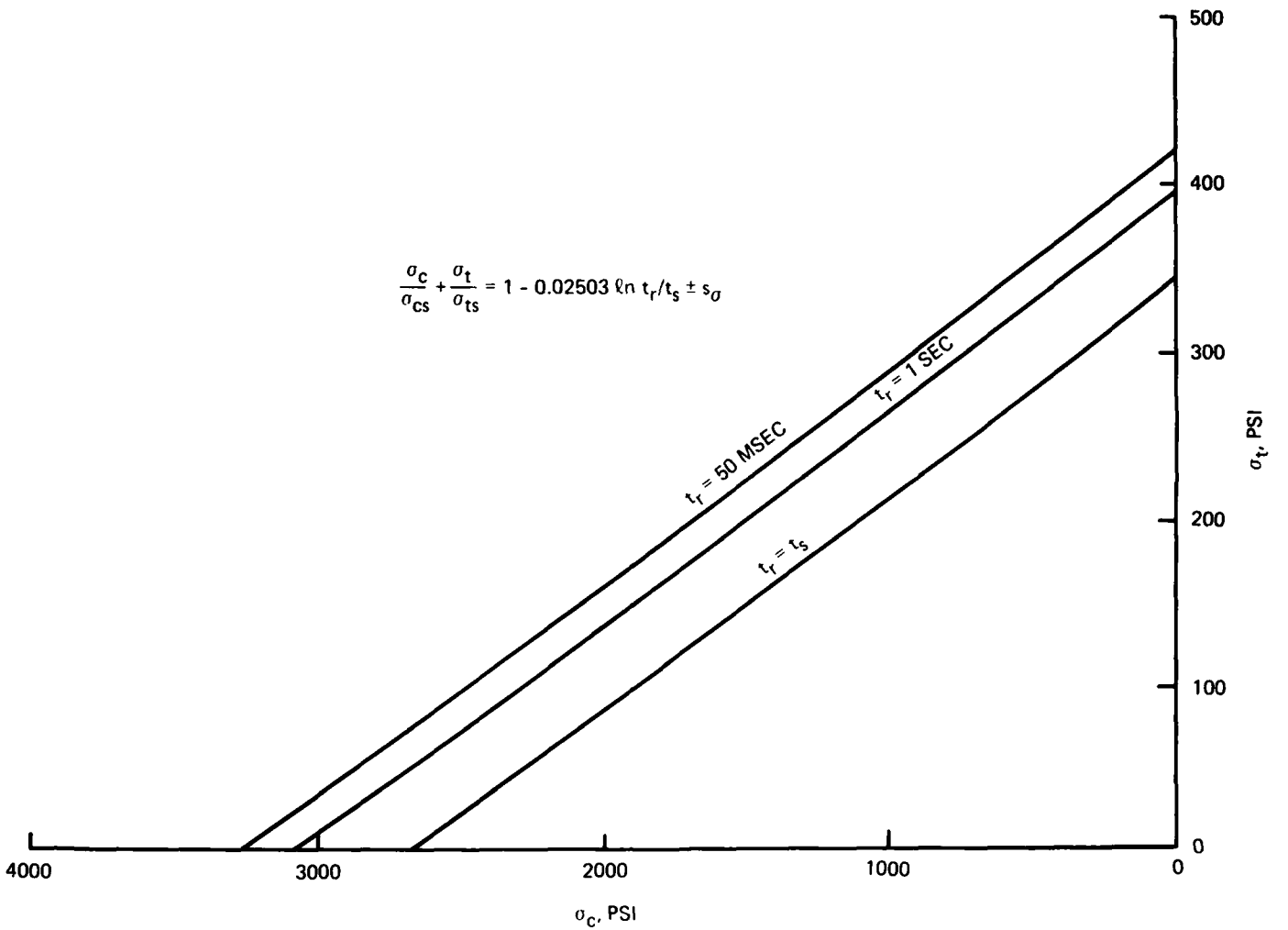

Figure 4.7 Dynamic biaxial concrete strength.

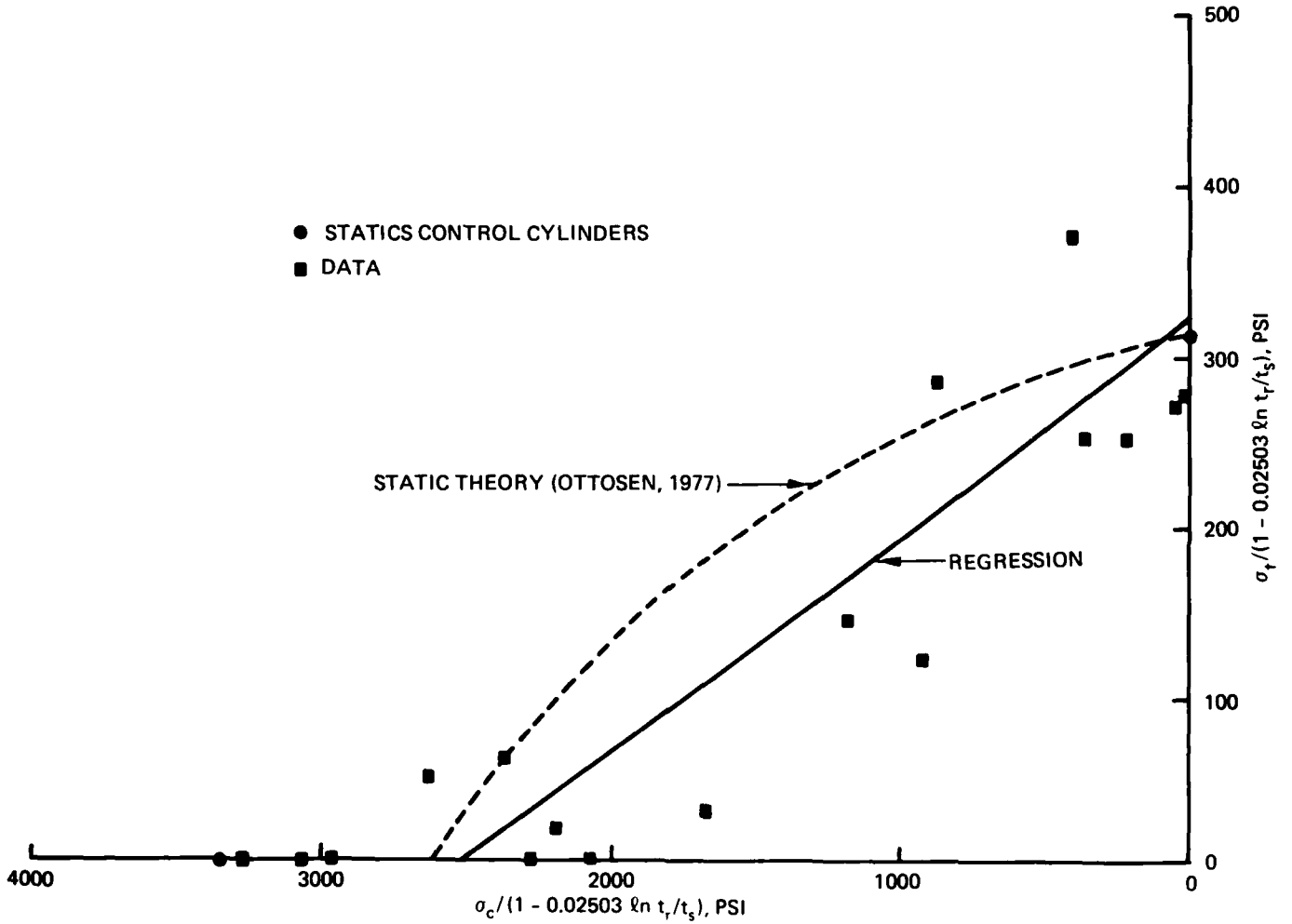

Figure 4.8 Biaxial dependence of dynamic strength.

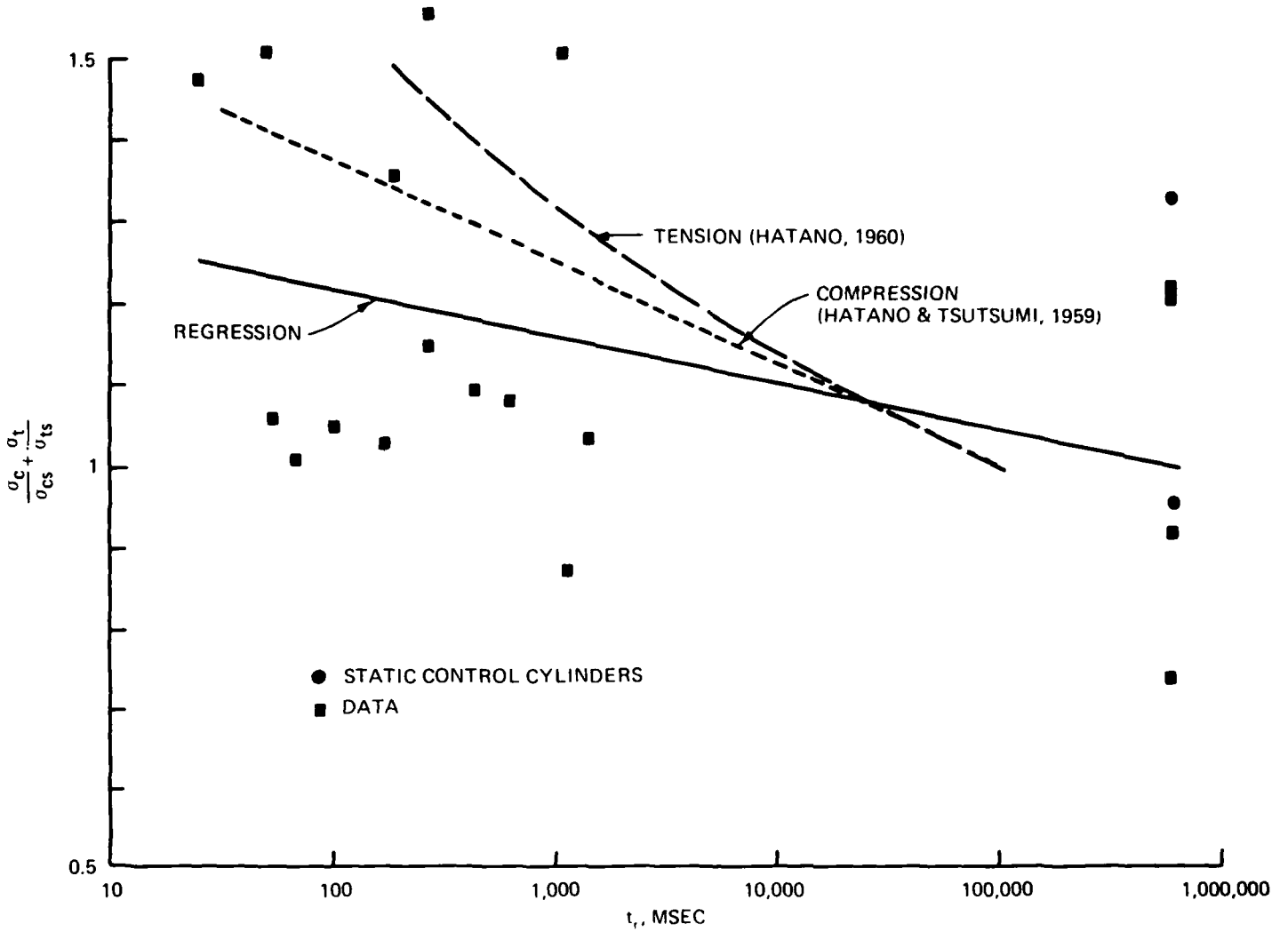

Figure 4.9 Dynamic dependence of biaxial strength.

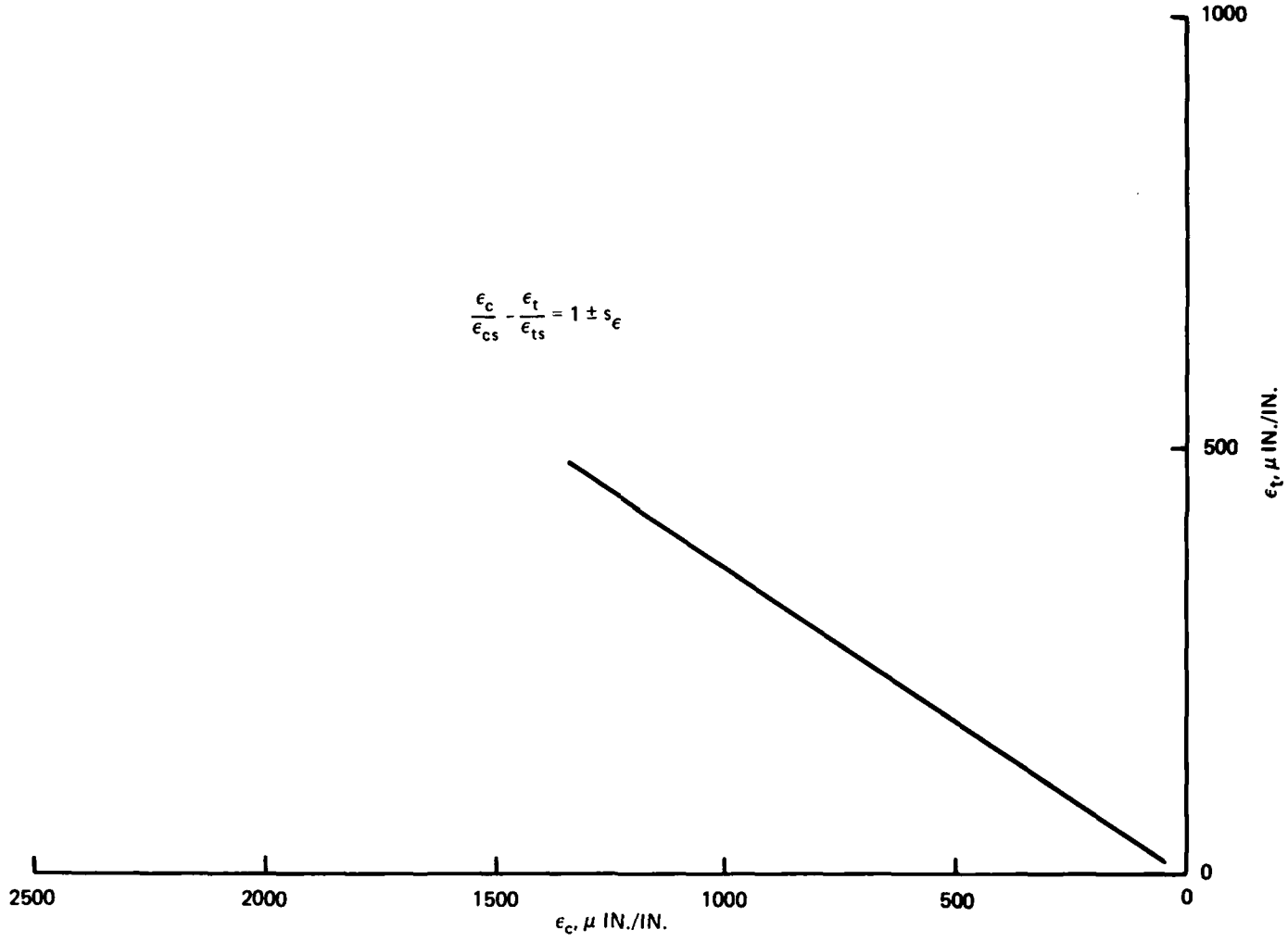

Figure 4.10 Dynamic biaxial strain-at-failure.

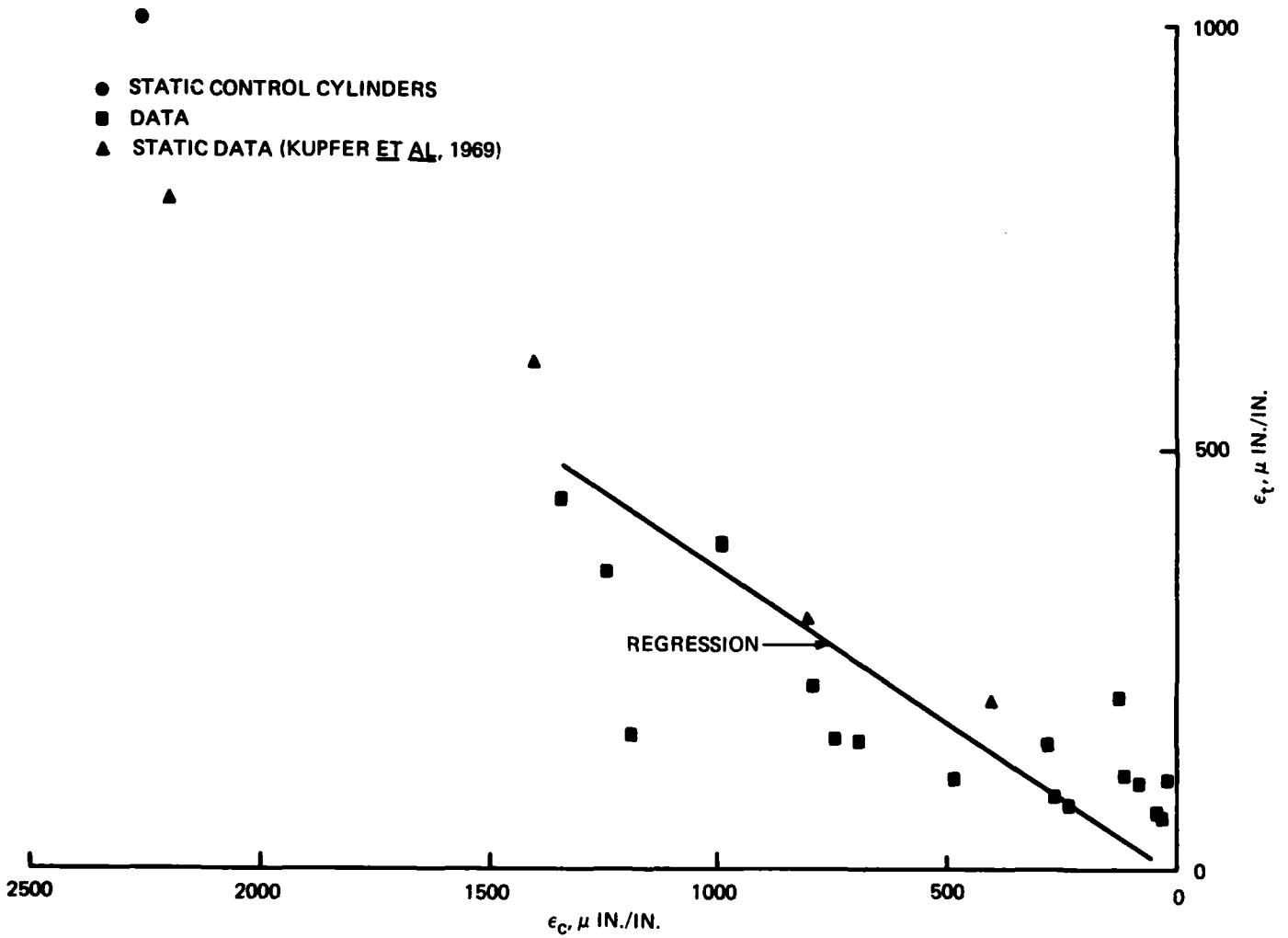

Figure 4.11 Biaxial dependence of dynamic strain-at-failure.

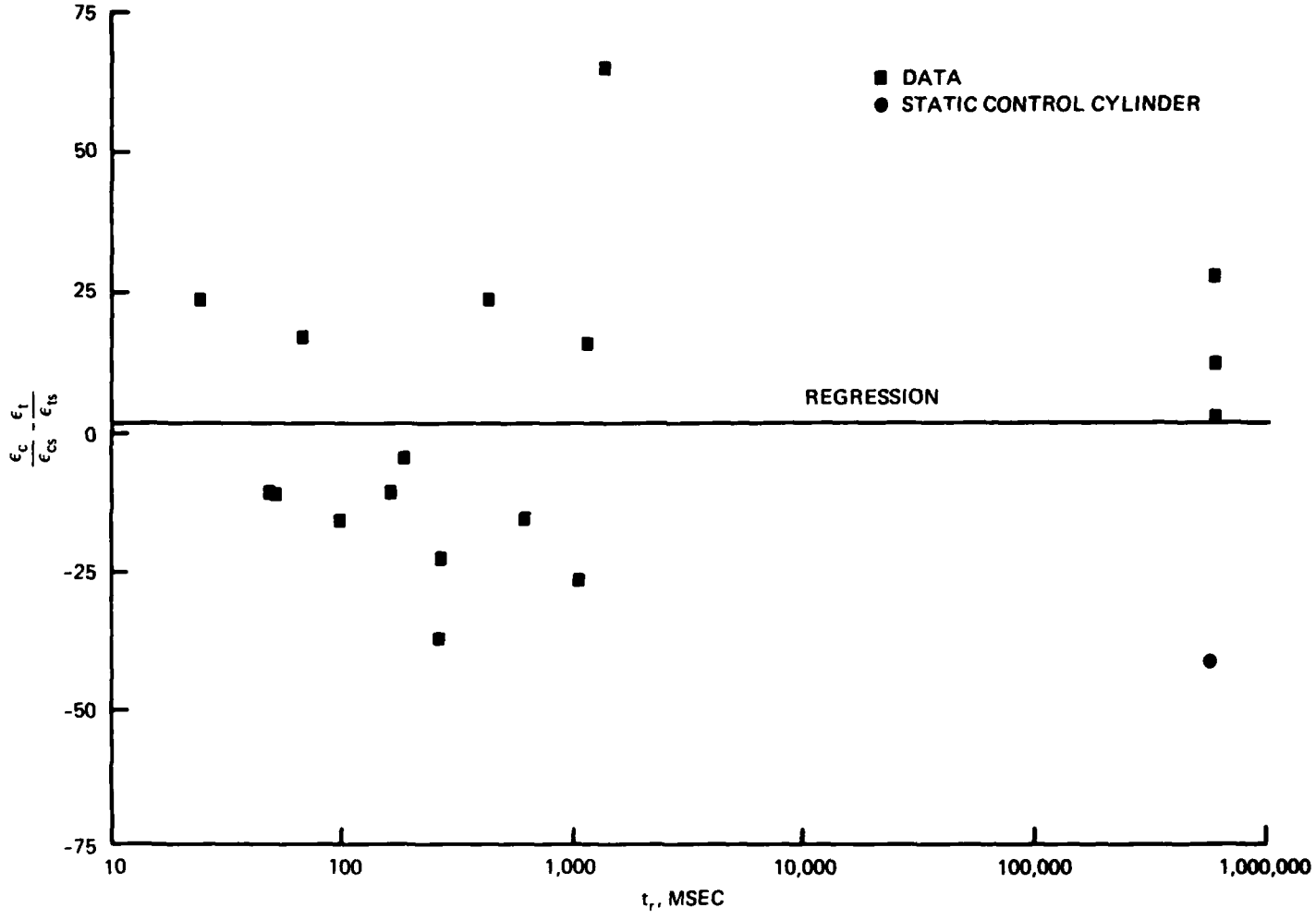

Figure 4.12 Dynamic independence of biaxial strain-at-failure.

CHAPTER 5

CONCLUSIONS

The tensile-compressive behavior of concrete in monotonically dynamic stress states can be investigated with a hollow cylindrical specimen subjected to axial and internal pressure loads by a large, open-loop hydraulic device.

Under combined dynamic loading, the tensile stress-at-failure decreases as the simultaneously acting compressive stress is increased.

For tensile-compressive loading, the strength increases as the stresses are applied more rapidly while the strains-at-failure remain constant with respect to loading time.

The stress-strain behavior of concrete under dynamic biaxial loading is more complex than the linearly elastic behavior assumed in seismic design analyses.

REFERENCES

American Concrete Institute. 1963. Symposium on Mass Concrete, SP-6, Detroit, 440 pp.

American Concrete Institute Committee 207. 1970. "Mass Concrete for Dams and Other Massive Structures," ACI Journal Proceedings, Vol 67, No. 4, pp 273-309.

American Society for Testing and Materials. 1972. Standard Test Method for Compressive Strength of Cylindrical Concrete Specimens, Designation: C 39-72, Philadelphia, Pa.

American Society for Testing and Materials. 1978. Standard Test Method for Direct Strength of Intact Rock Core Specimens, Designation: D 2936-78, Philadelphia, Pa.

Atchley, B. L. and Furr, H. L. 1967. "Strength and Energy Absorption Capabilities of Plain Concrete Under Dynamic and Static Loadings," ACI Journal, Proceedings Vol 64, No. 11, pp 745-756.

Balsara, J. P. and Hossley, J. R. 1973. "Evaluation of Safeguard System Perimeter Acquisition Radar Building Shear Key Connections," Technical Report N-73-9, U. S. Army Engineer Waterways Experiment Station, CE, Vicksburg, Miss.

Ban, S. and Muguruma, H. 1960. "Behavior of Plain Concrete Under Dynamic Loading with Straining Rate Comparable to Earthquake Loading," Proceedings of the Second World Conference on Earthquake Energy, Vol III, pp 1979-1993.

Bazant, Z. P. and Oh, B. H. 1982. "Strain-Rate Effect in Rapid Triaxial Loading of Concrete," J Engr Mech Div ASCE, Vol 108, No. EM5, pp 764-783.

Bresler, B. and Pister, K. S. 1958. "Strength of Concrete Under Combined Stresses," ACI Journal, Proceedings Vol 55, No. 3, pp 321-345.

Chen, A. C. T. and Chen, W. F. 1975. "Constitutive Relations for Concrete," J Engr Mech Div., ASCE, Vol 101, No. EM4, pp 465-481.

Chopra, A. K. 1978. "Earthquake Resistant Design of Concrete Gravity Dams," J Str Div, ASCE, Vol 104, No. ST6, pp 953-971.

Draper, N. R. and Smith, H. 1966. Applied Regression Analysis, Wiley, N. Y.

Goode, C. D. and Helmy, M. A. 1967. "The Strength of Concrete Under Combined Shear and Direct Stress," Magazine of Concrete Research (London), Vol 19, No. 59, pp 105-112.

Hatano, T. 1960. "Dynamical Behavior of Concrete Under Impulsive Tensile Load," Technical Report C-6002, Tokyo, Central Research Institute of the Electric Power Industry.

Hatano, T. and Tsutsumi, H. 1959. "Dynamical Compressive Deformation and Failure of Concrete Under Earthquake Load," Proceedings of the Second World Conference on Earthquake Engineering, Vol 3, Japan, pp 1979-1993.

Hatano, H. and Watanabe, H. 1971. "Fatigue Failure of Concrete Under Periodic Compressive Load," Trans Japanese Soc Civil Engrs, Vol 3, Part 1, pp 106-107.

Kirillov, A. P. 1977. "Strength of Concrete Under Seismic Loads," Translation of special protocol item under joint US-USSR project "Dams in Seismic Areas," U. S. Department of the Interior, Bureau of Reclamation, Denver, Colo

Kupfer, H., Hilsdorf, H. K., and Rusch, H. 1969. "Behavior of Concrete Under Biaxial Stresses," Journal of the American Concrete Institute, Vol 66, No. 8, pp 656-666.

McHenry, D. and Karni, J. 1958. "Strength of Concrete Under Combined Tension and Compressive Stresses," ACI Journal Proceedings, Vol 55, No. 10, pp 829-840.

Ottosen, N. S. 1977. "A Failure Criterion for Concrete," J Engr Mech Div ASCE, Vol 103, No. EM4, pp 527-535.

Pal, N. 1974. "Nonlinear Earthquake Response of Concrete to Gravity Dams," Report No. EERC 74-14, University of California.

Raphael, J. M. 1975. "Big Tujunga Dam, Strength and Elasticity of Concrete in Dam," Structural Research Laboratory, University of California, Berkeley.

Saucier, K. L. 1977. "Dynamic Properties of Mass Concrete," Miscellaneous Paper C-77-6, U. S. Army Engineer Waterways Experiment Station, CE, Vicksburg, Miss.

Takeda, J. and Tachikawa, H. 1973. "Deformation and Fracture of Concrete Subjected to Dynamic Load," Proceedings International Conference of Mechanical Behavior of Materials, Vol IV, Japan, pp 267-277.

Timoshenko, S. 1941. Strength of Materials, Part II Advanced Theory and Problems, 2nd ed, Van Nostrand, N. Y.

Watstein, D. 1953. "Effect of Straining Rate on the Compressive Strength and Elastic Properties of Concrete," ACI Journal, Proceedings Vol 49, No. 8, pp 729-744.